NASA TECHNICAL NOTE

NASA TN D-8180

NASA TN D-8180

OPTIMALITY STUDY OF A GUST ALLEVIATION SYSTEM FOR LIGHT WING-LOADING STOL AIRCRAFT

Masaki Komoda

Ames Research Center
Moffett Field, Calif. 94035

NATIONAL AERONAUTICS AND SPACE ADMINISTRATION • WASHINGTON, D. C. • FEBRUARY 1976

1. Report No. NASA TN D-8180	2. Government Accession No.	3. Recipient's Catalog No.
4. Title and Subtitle OPTIMALITY STUDY OF A GUST ALLEVIATION SYSTEM FOR LIGHT WING-LOADING STOL AIRCRAFT		5. Report Date February 1976
		6. Performing Organization Code
7. Author(s) Masaki Komoda		8. Performing Organization Report No. A-5906
		10. Work Unit No. 505-06-92
9. Performing Organization Name and Address Ames Research Center, NASA Moffett Field, Calif. 94035		11. Contract or Grant No.
		13. Type of Report and Period Covered Technical Note
12. Sponsoring Agency Name and Address National Aeronautics and Space Administration Washington, D. C. 20546		14. Sponsoring Agency Code

15. Supplementary Notes

The author was an NRC Postdoctoral Research Associate at Ames Research Center.

16. Abstract

An analytical study was made of an optimal gust alleviation system that employs a vertical gust sensor mounted forward of an aircraft's center of gravity. Frequency domain optimization techniques were employed to synthesize the optimal filters that process the corrective signals to the flaps and elevator actuators. Special attention was given to evaluating the effectiveness of lead time, that is, the time by which relative wind sensor information should lead the actual encounter of the gust. The resulting filter is expressed as an implicit function of the prescribed control cost. A numerical example for a light wing-loading STOL aircraft is included in which the optimal trade-off between performance and control cost is systematically studied.

17. Key Words (Suggested by Author(s)) Gust alleviation		18. Distribution Statement Unclassified - Unlimited STAR Category - 08	
19. Security Classif. (of this report) Unclassified	20. Security Classif. (of this page) Unclassified	21. No. of Pages 61	22. Price* $4.25

* For sale by the National Technical Information Service, Springfield, Virginia 22161

SYMBOLS*

$A(s)$	system characteristics matrix in the Wiener-Hopf (W-H) equation, equation (22a)
a	positive real constant in first-order Padé expansion, equation (34)
$\mathbf{b}(s)$	forcing vector in W-H equation, equation (22b)
$C_{m_{\delta_e}}$	nondimensional stability derivative, $\frac{mk_y{}^2}{qSc} \cdot \frac{\partial M}{\partial \delta_e}$
$C(s)$	control system dynamics matrix, equation (9)
$C_{Z_{\delta_e}}$	nondimensional stability derivative, $\frac{mU}{qS} \cdot \frac{\partial Z}{\partial \delta_e}$.
c	aerodynamic chord of the wing, m
c_{g_e}	gain of equivalent deterministic disturbance, equation (19a)
$-c_\infty$	system pole corresponding to the control dynamics in limiting cases, equations (46) and (B11)
$\mathbf{c}_o, \mathbf{c}_w, \mathbf{c}_k$	gain vectors of filter, equation (29a)
$d_a(s)$	open-loop characteristic polynomial, $\prod_{i=1}^{i_a} (s + s_{ai})$
$d_{cf/e}(s)$	control system denominator, $\left(s + \mu_{f/e}\right)$
$d_u(s)$	system characteristic polynomial with feed-forward loop closed, $\prod_{k=1}^{k_u} (s + s_{uk})$
$e_n{}^*(s)$	$e_n(s)$ with replacement of RH zero by its image zero in LH s-plane, if any
e_{no}	leading term coefficient of $e_n(s)$
$e(s)$	δ_e-into-y transfer function, $\frac{e_n(s)}{d_a(s)}$
$F_a(s)$	$\boldsymbol{\delta}$-into-$\mathbf{x}$ transfer function matrix, $\frac{F_{an}(s)}{d_a(s)}$, equations (1) and (4)

*Symbols used only in the appendices are not included in this list.

$f(s)$	δ_f-into-y transfer function, $\frac{f_n(s)}{d_a(s)}$
$\mathbf{f}(s)$	$\boldsymbol{\delta}$-into-y transfer function vector, $\frac{\mathbf{f}_n(s)}{d_a(s)}$, equations (5) and (6)
$G_a(s)$	$\mathbf{w}_g$-into-$\mathbf{x}$ transfer function matrix, $\frac{G_{an}(s)}{d_a(s)}$, equations (1) and (4)
g	gravitational constant, m/sec^2
$g_n{}^*(s)$	numerator polynomial defined by equation (B20)
$g(s)$	w_g-into-y transfer function, $\frac{g_n(s)}{d_a(s)}$, equations (5) and (6)
$g_u(s)$	system transfer function w_g-into-y when feed-forward loop is closed, $g_{uo}(s) + g_{up}(s)$
$g_{uo}(s)$, $g_{up}(s)$	parts of $g_u(s)$ due to basic part of filter $\mathbf{k}_o(s)$ and additional part of filter $\mathbf{k}_p(s;\tau_g)$, respectively, equations (C33) and (C35)
$\mathbf{g}_a(s)$	any column of $G_a(s)$
$\mathbf{h}(s)$	output defining vector, equation (5)
i_a	order of polynomial $d_a(s)$
J	augmented performance index, equation (15)
J_{uf}, J_{ue}	cost indices, equations (10) and (16b)
J_y	performance index, equations (8) and (16a)
j	$\sqrt{-1}$
$\mathbf{k}(s)$	optimal filter, $w_g(s)e^{\tau_g s}$-into-$\mathbf{u}(s)$, equation (13)
$\mathbf{k}_o(s)$	basic part of $\mathbf{k}(s)$, or $\mathbf{k}(s)$ when $\tau_g = 0$, equation (33)
$\mathbf{k}_p(s;\tau_g)$	additional part of $\mathbf{k}(s)$ when $\tau_g > 0$, equation (33)
k_u	order of polynomial $d_u(s)$
k_y	radius of gyration about lateral body axis, m
L	turbulence scale length in one-dimensional Dryden model, m
$\mathcal{L}^{-1}[\ ]$	inverse Laplace transform of [ ]

l_c fuselage station measured rearward from CG, m

l_{cc} center of percussion with respect to elevator measured rearward from CG, equation (42), m

l_g location of vane measured forward from CG, m

l_T tail moment arm, m

$\mathbf{l}_k, \tilde{\mathbf{l}}$ filter gain of constant part, equation (32a), and its suboptimal, equation (36)

M_q pitching moment derivative, $\frac{1}{mk_y{}^2} \cdot \frac{\partial M}{\partial \dot{\theta}}$, 1/sec

M_u pitching moment derivative, $\frac{1}{mk_y{}^2} \cdot \frac{\partial M}{\partial u}$, 1/sec·m

M_α pitching moment derivative, $\frac{1}{mk_y{}^2} \cdot \frac{\partial M}{\partial \alpha}$, 1/sec^2

$M_{\dot{\alpha}}$ pitching moment derivative, $\frac{1}{mk_y{}^2} \cdot \frac{\partial M}{\partial \dot{\alpha}}$, 1/sec

M_{δ_e} pitching moment derivative, $\frac{1}{mk_y{}^2} \cdot \frac{\partial M}{\partial \delta_e}$, 1/sec^2

M_{δ_f} pitching moment derivative, $\frac{1}{mk_y{}^2} \cdot \frac{\partial M}{\partial \delta_f}$, 1/sec^2

$M_{\dot{\delta}_f}$ pitching moment derivative, $\frac{\varepsilon_{\delta_f}}{\varepsilon_\alpha} M_{\dot{\alpha}}$, 1/sec

m mass of airplane, kg

n_z normal acceleration factor at fuselage station l_c, g

$P(s)$ factored matrix of $A(s)$, equation (B4)

$\mathbf{p}_{on}(s)$ numerator polynomial vector of $\mathbf{k}_o(s)$, equation (29)

$\mathbf{r}_k, \tilde{\mathbf{r}}$ filter gain of $s = s_{uk}$ part, equation (32a), and its suboptimal, equation (36)

S wing area, m^2

s complex frequency, rad/sec

$-s_{ai}$	ith pole of open loop system, rad/sec
$-s_{uk}$	kth pole of system with feed-forward loop closed, rad/sec
$\mathbf{s}_k, \tilde{\mathbf{s}}_k$	filter gain of $s = -s_{uk}$ part, equation (32a), and its suboptimal, equation (36)
t	time, sec
$\mathbf{t}_k, \tilde{\mathbf{t}}$	filter gain of $s = -w_g/\sqrt{3}$ part, equation (32a), and its suboptimal, equation (36)
U	trimmed airspeed, m/sec
u_e	input to elevator actuation system, deg
u_f	input to flap actuation system, deg
$u_g(s)$	horizontal component of gust, m/sec
$\mathbf{u}(s)$	hypothetically inertialess control input vector, equation (9)
$u(s)$	longitudinal perturbation velocity, m/sec
$\mathbf{v}(s)$	equivalent optimal control, $[v^f(s),v^e(s)]^T = \mathbf{k}(s)w_{g_e}^{-1}(s)$, equation (24)
$\mathbf{v}_o(s)$	basic part of $\mathbf{v}(s)$ when $\tau_g = 0$, equation (24)
$\mathbf{v}_p(s;\tau_g)$	additional part of $\mathbf{v}(s)$ when $\tau_g > 0$, equation (24)
$w_g(s)$	vertical component of gust, m/sec
$w_{g_e}(s)$	equivalent deterministic disturbance, equation (19)
$\mathbf{w}_g(s)$	turbulence vector evaluated at CG, $[u_g(s),w_g(s)]^T$
X_u	longitudinal force derivative, $\frac{1}{m} \cdot \frac{\partial X}{\partial u}$, 1/sec
X_α	longitudinal force derivative, $\frac{1}{m} \cdot \frac{\partial X}{\partial \alpha}$, m/sec^2
X_{δ_e}	longitudinal force derivative, $\frac{1}{m} \cdot \frac{\partial X}{\partial \delta_e}$, m/sec^2
X_{δ_f}	longitudinal force derivative, $\frac{1}{m} \cdot \frac{\partial X}{\partial \delta_f}$, m/sec^2
$\mathbf{x}(s)$	state variable, $[u(s),\alpha(s),\theta(s)]^T$, equation (1)
$y(s)$	output variable, equation (5)

Z_u	vertical force derivative, $\frac{1}{mU} \cdot \frac{\partial Z}{\partial u}$, 1/m
Z_α	vertical force derivative, $\frac{1}{mU} \cdot \frac{\partial Z}{\partial \alpha}$, 1/sec
Z_{δ_e}	vertical force derivative, $\frac{1}{mU} \cdot \frac{\partial Z}{\partial \delta_e}$, 1/sec
Z_{δ_f}	vertical force derivative, $\frac{1}{mU} \cdot \frac{\partial Z}{\partial \delta_f}$, 1/sec
z_e	RH zero in $e(s)$, if any
$\mathbf{z}(s)$	coefficient vector defining first variation of J, equation (21)
$\alpha(s)$	perturbed angle of attack due to inertial velocity, rad
β_{ok},β_{pk}	gain vectors of $\mathbf{v}_p(s;\tau_g)$ for $s = s_{uk}$, equations (C20) and (C21), also equations (C28a) and (C28b)
$\gamma^f_{pe},\gamma^f_{p\mu}$	filter gains in flap system corresponding to the limiting case $\sqrt{\bar{u}_e^2} \to \infty$, equation (49)
$\boldsymbol{\gamma}_{ok},\boldsymbol{\gamma}_{pk}$	gain vectors of $\mathbf{v}(s)$ for $s = -s_{uk}$, equations (C28a) and (C28b)
$\delta_e(s)$	elevator deflection, rad or deg
$\delta_f(s)$	flap deflection, rad or deg
$\boldsymbol{\delta}(s)$	control surface deflection vector, $[\delta_f(s),\delta_e(s)]^T$, rad or deg
$\varepsilon_\alpha,\varepsilon_{\delta_f}$	downwash angle slope due to wing and flap
η_1,η_2	gain vectors of $\mathbf{v}(s)$ for $s = -\omega_g$, equation (C27)
$\theta(s)$	perturbed pitch attitude, rad
Λ	multiplier matrix, equation (17)
$\lambda_f{}^2,\lambda_e{}^2$	Lagrange's multipliers for $\bar{u}_f{}^2$ and $\bar{u}_e{}^2$
$\frac{1}{\mu_f}, \frac{1}{\mu_e}$	equivalent first-order time constant for flap and elevator control system, sec
ν	constant defined in equation (B7)
ρ_e,ρ_{ef}	system gain for $\lambda_e \to 0$, equations (39) and (55)

$\rho(s)$	complemental part of filter, $[\rho^f(s),\rho^e(s)]^T$, equations (C9) and (C21)
σ	real part of s
σ_g	rms intensity of turbulence, m/sec, $\left[\int_o^\infty \Phi_{w_g}(\omega)d\omega\right]^{1/2}$
τ_g	lead time, $\frac{l_g}{U}$, sec
$\Phi(\omega)$	power sepctrum of $\mathbf{w}_g$, $diag[\Phi_{u_g}(\omega),\Phi_{w_g}(\omega)]$, equation (3)
$\Phi_{n_z}(\omega)$	power spectrum of n_z, equation (56)
ω	angular frequency, rad/sec
ω_g	gust frequency, $\frac{U}{L}$, rad/sec
ω_{u_g}	longitudinal gust frequency, $\xi\omega_g$, where ξ is a factor indicating approximate nonisotropy near the ground, rad/sec

Notation:

$\overline{(\ )}$	mean square value of ( ), or if ( ) is a polynomial in s, $\overline{(\ )}$ indicates $-s$ is substituted for s
$(\ )^T$	transpose of (matrix)
$(\ )^{-1}$	inverse of (matrix)
$\tilde{(\ )}$	suboptimal of ( )
$\dot{(\ )}$	time derivative of ( )
$(\ )_n$	numerator of (rational polynomial)
$(\ )_o$	basic part of ( )
$(\ )_p$	additional part of ( )
$[\ ]_\pm$	that portion of [ ] which is analytic in RH/LH s-plane, respectively

OPTIMALITY STUDY OF A GUST ALLEVIATION SYSTEM FOR LIGHT WING-LOADING STOL AIRCRAFT

Masaki Komoda*

Ames Research Center

SUMMARY

An analytical study was made of an optimal gust alleviation system that employs a vertical gust sensor mounted forward of an aircraft's center of gravity. Frequency domain optimization techniques were employed to synthesize the optimal filters that process the corrective signals to the flaps and elevator actuators. Special attention was given to evaluating the effectiveness of lead time, that is, the time by which relative wind sensor information should lead the actual encounter of the gust. The resulting filter is expressed as an implicit function of the prescribed control cost. A numerical example for a light wing-loading STOL aircraft is included in which the optimal trade-off between performance and control cost is systematically studied.

INTRODUCTION

The need for gust alleviation in reducing peak loads and improving ride quality has been apparent since the early days of aviation, and numerous studies of alleviation techniques have been conducted. A review of a number of these efforts and of the specific problems associated with gust alleviation is given in reference 1. In the last few years, the need to improve ride quality for light wing-loading STOL aircraft in short-haul service has led to increased interest in gust alleviation systems. Analysis has shown that the severe disturbances in the longitudinal mode arising from vertical gusts can be effectively alleviated through the use of direct-lift devices, such as flaps, as the primary control (refs. 2-5), and that systems that employ relative wind sensors in conjunction with inertial sensors (ref. 6) are more attractive than other types. The use of a relative wind sensor permits the gust velocity component to be extracted as a disturbance signal so that a feedforward loop can be constructed that does not interfere with the pilot's control of the aircraft. This arrangement also permits the use of gust signals with positive lead time (see fig. 1).

In most analyses of gust alleviation systems, the filter that lies between the sensors and the control actuators has been assumed to be of fixed shape and optima have been defined through variation of system parameters such as filter gains. Some alleviation system studies have been made in which the filter shape is not assumed, but is optimized using frequency domain analysis (refs. 7 and 8). In any practical system, control cost, such as surface

*NRC Postdoctoral Research Associate at Ames Research Center. Presently, National Aerospace Laboratory, Mitaka, Tokyo, Japan

deflection or deflection rate, has some limit. Since limited cost results in limited performance, it is of interest to examine how the use of an optimally filtered lead signal improves system performance.

The present analysis extends the frequency domain optimization technique to define optima for systems with a feed-forward loop with lead time provided by a relative wind sensor located forward of the aircraft's center of gravity. A numerical example is given, for a light wing-loading STOL aircraft, that illustrates the effectiveness of lead time in reducing control cost for systems that use flaps alone, elevator alone, and combinations of flap and elevator.

DESCRIPTION OF SYSTEM

Major Assumptions

The objective of this analysis is to improve aircraft ride quality. Vertical acceleration disturbances within a frequency band of approximately 0.2 to 20 Hz are of particular importance from a ride-quality standpoint (ref. 9). Analyses covering this frequency band require the inclusion of unsteady aerodynamic effects and elastic modes in the state equation. These effects are omitted in this analysis for reasons of simplicity. Even for large and flexible aircraft, however, the rigid body modes make a fundamental contribution to the total vertical acceleration disturbance; therefore this study should give a good indication of the possible ride-quality improvements.

Spanwise variation of the vertical gusts is also ignored in this analysis. This may have a significant effect on the system performance (ref. 10) and should be considered in future extensions of this work. In addition, future studies should include the synthesis of the optimal system which gives the best estimate of the equivalent one-dimensional gust component under the presence of measurement noise.

Airplane Dynamics and Turbulence Modeling

Linear perturbation equations are assumed to describe the rigid body response of the airplane both as to control surface deflection and atmospheric turbulence. Considering a particular realization of turbulence which is temporarily assumed to vanish outside a long but finite time interval $|t| \leq T/2$

$$\mathbf{x}(s) = F_a(s)\boldsymbol{\delta}(s) + G_a(s)\mathbf{w}_g(s) \tag{1}$$

is obtained after bilateral Laplace transform using complex frequency s, where $\mathbf{x} = (u,\alpha,\theta)^T$ is state, $\boldsymbol{\delta} = (\delta_f,\delta_e)^T$ is control surface deflection, $\mathbf{w}_g = (u_g,w_g)^T$ is longitudinal mode disturbance, and F_a and G_a are corresponding matrix transfer functions with consistent dimensions. Appendix A summarizes the expressions for $F_a(s)$ and $G_a(s)$.

The spacewise wave form of a frozen turbulence is approximated at each instant by a "linear representation." That is, the velocity component itself and only the linear part of spacewise variations of turbulence, both evaluated at CG, are considered. Thus, the rigid body aerodynamic derivatives are consistent in constructing $G_a(s)$.

Since rigid body response is the primary concern in this study, no flexible mode is considered. By the same token, no unsteady aerodynamic effects are included. However, by incorporating the lift growth functions such as Wagner's and Küssner's, into $F_a(s)$ and $G_a(s)$, the refinement necessary to consider unsteady effects could be readily made.

The disturbance power spectrum is given by

$$\Phi(\omega) = \frac{1}{\pi}\int_{-\infty}^{\infty} E\left[\lim_{T\to\infty}\frac{1}{T}\int_{-T/2}^{T/2} \mathbf{w}_g(t)\mathbf{w}_g^T(t + \tau)dt\right]e^{-j\omega\tau}\, d\tau \tag{2}$$

where ω is the angular frequency, $\mathbf{w}_g(t)$ is a realization of turbulence, and where E stands for the ensemble average of turbulence. Although the existence of cross power spectra and their effect upon airplane response are suggested, especially near the ground (ref. 11), only diagonal elements of $\Phi(\omega)$ are retained. A one-dimensional Dryden model of continuous turbulence is used in the analysis. The one-sided power spectra are given by

$$\begin{aligned}\Phi(\omega) &= diag[\Phi_{u_g}(\omega)\ ,\quad \Phi_{w_g}(\omega)] \\ &= \frac{\omega_g\sigma_g^2}{\pi}\, diag\left[\frac{2}{\omega^2 + \omega_{ug}^2},\quad \frac{3\omega^2 + \omega_g^2}{(\omega^2 + \omega_g^2)^2}\right]\end{aligned} \tag{3}$$

where gust frequency, $\omega_g = U/L$, and rms intensity, σ_g, are the primary parameters. Excluding off-diagonal terms in $\Phi(\omega)$ simplifies the optimization process because this separates the effects of u_g and w_g, and the results thereof are additive. Since a similar formulation is valid for the u_g component, only w_g is considered in the following formulation. The term $G_a(s)\mathbf{w}_g(s)$ in equation (1) is thus replaced by $\mathbf{g}_a(s)w_g(s)$, where $\mathbf{g}_a(s)$ is the column of $G_a(s)$.

By ignoring unsteady lift growth effects and using a linear representation for turbulence with a one-dimensional power spectrum, a trivial difficulty is introduced in the construction of F_a and G_a, if a conventional approximation $e^{-z} \doteqdot (1 - z)$ is used for the down-wash and gust-wash lags (see eq. (A3)). These assumptions lead to an erroneously high response in the high frequency range. Actually, high frequency spectra of $F_a(s)\boldsymbol{\delta}(s)$ and $G_a(s)\mathbf{w}_g(s)$ are attenuated by both unsteady effects and spanwise variations of turbulence. To avoid this difficulty, while keeping a reasonable simplicity in the optimization procedure, the first-order Padé expansion, $e^{-z} \doteqdot (-z + 2)/(z + 2)$, is used to approximate these lags.

Under the assumptions stated above, the transfer function matrices $F_a(s)$ and $G_a(s)$ have a common denominator $d_a(s)$, that is the open loop characteristic equation. A stable open loop is assumed. Denoting by $F_{an}(s)$ and $G_{an}(s)$ the numerator matrices of $F_a(s)$ and $G_a(s)$, respectively,

$$F_a(s) = \frac{F_{an}(s)}{d_a(s)}, \qquad G_a(s) = \frac{G_{an}(s)}{d_a(s)} \tag{4}$$

each entry of F_{an} and G_{an} is a polynomial in s with an order not greater than that of $d_a(s)$.

Output Variable and Performance Index

Suppose a scalar output variable $y(s)$ is taken as the basis for assessing ride qualities, where $y(s)$ is defined by

$$\begin{aligned} y(s) &= \mathbf{h}^T(s)\mathbf{x}(s) \\ &= \mathbf{f}^T(s)\boldsymbol{\delta}(s) + g(s)w_g(s) \end{aligned} \tag{5}$$

with

$$\left.\begin{aligned} \mathbf{f}^T(s) &\triangleq \mathbf{h}^T(s)F_a(s) & \qquad g(s) &\triangleq \mathbf{h}^T(s)\mathbf{g}_a(s) \\ &\triangleq [f(s), e(s)] & &= \frac{g_n(s)}{d_a(s)} \\ &= \frac{[f_n(s), e_n(s)]}{d_a(s)} & & \end{aligned}\right\} \tag{6}$$

The output-defining vector $\mathbf{h}(s)$ is a polynomial in s. For example, if $y(s)$ is the normal acceleration factor n_z at a fuselage station l_c (positive when rearward), then

$$\mathbf{h}^T(s) = \frac{U}{g}\left(0,\ -s,\ s - \frac{l_c}{U}\, s^2\right) \tag{7}$$

In the case when $y(s)$ is not a simple dynamic quantity but is, as an example, a bandpass filtered one, $\mathbf{h}(s)$ might be a rational polynomial in s. Additional poles would hence be included in $\mathbf{f}^T(s)$ and $g(s)$.

Since reasonable grounds for choosing otherwise in assessing ride qualities are lacking, the simple mean square value, $\overline{y^2}$, is chosen as a performance index, J_y. Using the general transfer function $y(s)/w_g(s)$, the performance index is then

$$J_y \triangleq \overline{y^2} = \frac{1}{2}\int_{-\infty}^{\infty} \left|\frac{y}{w_g}(j\omega)\right|^2 \Phi_{w_g}(\omega)\,d\omega \tag{8}$$

As is well known, the mean square, or equivalent, the rms, value of a random process can be related to other measures of the process such as the probability of exceeding a given level, even if the process is not Gaussian (ref. 12). In any case, the vector $\mathbf{h}(s)$ must be so chosen that J_y is well defined by equation (8).

Control Surface Dynamics and Cost Index

The control surface dynamics are generally written as

$$\boldsymbol{\delta}(s) = C(s)\mathbf{u}(s) \tag{9}$$

where $\mathbf{u} = (u_f, u_e)^T$ is a hypothetically inertialess control input to the actuating system, and $C(s)$ is the corresponding transfer function matrix. It would be reasonable enough to define the cost indices J_{uf} and J_{ue} by

$$J_{u_{f/e}} = \bar{u}^2_{f/e} = \frac{1}{2}\int_{-\infty}^{\infty} \left|\frac{u_{f/e}}{w_g}(j\omega)\right|^2 \Phi_{w_g}(\omega)\,d\omega \tag{10}$$

where $\bar{u}_f{}^2$ and $\bar{u}_e{}^2$ are the mean square input values of the flap and elevator actuating system and $u_{f/e}(s)/w_g(s)$ are corresponding transfer functions.

Instead of trying to model actual systems precisely, a first-order decoupled dynamic system is assumed for $C(s)$ in the analysis. Thus,

$$C(s) = diag\left(\frac{\mu_f}{s+\mu_f}, \frac{\mu_e}{s+\mu_e}\right) \tag{11}$$

where μ_f and μ_e are non-negative real, and distinct. Using equations (11) and (9), equation (10) becomes

$$\begin{aligned} J_{u_{f/e}} &= \bar{u}^2_{f/e} = \frac{1}{2}\int_{-\infty}^{\infty} \left|\frac{j\omega + \mu_{f/e}}{\mu_{f/e}}\frac{\delta_{f/e}}{w_g}(j\omega)\right|^2 \Phi_{w_g}(\omega)\,d\omega \\ &= \bar{\delta}^2_{f/e} + \frac{\bar{\dot{\delta}}^2_{f/e}}{\mu^2_{f/e}} \end{aligned} \tag{12}$$

which indicates that the cost index defined above affords a good measure of the mean square values of control surface deflection and its time rate.

Control Law

One of the basic assumptions of this study is that an instantaneous measurement of disturbance $\mathbf{w}_g$ is available with some lead time $\tau_g(>0)$. The simplest way to measure the disturbance before it actually hits the lifting surfaces would be a combination of a relative wind sensor, mounted ahead of the wing, and inertial sensors that generate signals due to non-gust relative wind components. Although it is necessary to examine carefully the possible adverse effect due to measurement noise, more sophisticated versions, such as a predicting filter, could be utilized to increase the lead time τ_g.

Let it be assumed that there exists an optimal filter $\mathbf{k}(s)$ such that a control law

$$\mathbf{u}(s) = -\mathbf{k}(s)w_g(s)e^{\tau_g s} \tag{13}$$

minimizes the performance index J_y subject to the prescribed cost indices J_{uf} and J_{ue}. Only asymptotic stability and causality are required for $\mathbf{k}(s)$ at this stage. Successive substitutions of equation (13) into (9), and of equation (9) into (5), give the system transfer function with feed-forward loop closed,

$$\begin{aligned} y(s) &= g_u(s)w_g(s) \\ &= [g(s) - \mathbf{f}^T(s)C(s)\mathbf{k}(s)e^{\tau_g s}]w_g(s) \end{aligned} \tag{14}$$

Equations (13) and (14) are valid for each realization $w_g(s)$.

OPTIMIZATION

Augmented Performance Index

Following standard procedures, an augmented performance index J is defined by

$$J = J_y + \lambda_f{}^2 J_{uf} + \lambda_e{}^2 J_{ue} \tag{15}$$

where λ_f and λ_e are real multipliers. After the substitutions of equations (14) and (13) into equations (8) and (10), respectively,

$$J_y = \frac{1}{2}\int_{-\infty}^{\infty} g_u(-j\omega)\Phi_{wg}(\omega)g_u(j\omega)\,d\omega \tag{16a}$$

$$\lambda_f{}^2 J_{uf} + \lambda_e{}^2 J_{ue} = \frac{1}{2}\,Tr\int_{-\infty}^{\infty} \Lambda\mathbf{k}(-j\omega)\mathbf{k}^T(j\omega)\Phi_{wg}(\omega)\,d\omega \tag{16b}$$

where

$$\Lambda = diag(\lambda_f{}^2, \lambda_e{}^2) \tag{17}$$

Using equations (16a) and (16b), equation (15) is expressed as a functional of the unknown filter $\mathbf{k}(j\omega)$.

Weiner-Hopf Equation

Instead of solving for $\mathbf{k}(s)$, it is more convenient to define and solve for a vector

$$\mathbf{v}(s) = \mathbf{k}(s) w_{g_e}(s) \tag{18}$$

where $w_{g_e}(s)$ is a factored form of $\Phi_{w_g}(\omega)$ in the complex s-plane, that is,

$$\Phi_{w_g}\left(\frac{s}{j}\right) = w_{g_e}(-s) w_{g_e}(s) \tag{19}$$

where, from equation (3),

$$w_{g_e}(s) \triangleq c_{g_e} \frac{s + \omega_g/\sqrt{3}}{(s + \omega_g)^2} \; ; \qquad c_{g_e} = \left(\frac{3\omega_g}{\pi}\right)^{1/2} \sigma_g \tag{19a}$$

which is usually referred to as the equivalent deterministic disturbance. As is known, the original (stochastic) problem of finding $\mathbf{k}(s)$ is equivalent to the deterministic problem of finding $\mathbf{v}(s)$ with respect to the same J. Once $\mathbf{v}(s)$ is found, $\mathbf{k}(s)$ is readily obtained by

$$\mathbf{k}(s) = \mathbf{v}(s) w_{g_e}^{-1}(s) \tag{20}$$

As derived in appendix B, the Wiener-Hopf (W-H) equation to solve is

$$[\mathbf{z}(s)]_+ \triangleq [A(s)\mathbf{v}(s) - \mathbf{b}(s)e^{-\tau_g s}]_+ = \mathbf{0} \tag{21}$$

where

$$A(s) \triangleq \Lambda + C(-s)\mathbf{f}(-s)\mathbf{f}^T(s)C(s) \tag{22a}$$

$$\mathbf{b}(s) \triangleq C(-s)\mathbf{f}(-s)g(s)w_{g_e}(s) \tag{22b}$$

and where $[\;]_+$ indicates that part of $[\;]$ which is analytic in the RH s-plane. Since the matrix $A(s)$ is real and positive on the imaginary axis of the s-plane, solution $\mathbf{v}(s)$ gives a minimum of J.

Solution $\mathbf{v}(s)$

As shown in appendix B, the equivalent optimal control $\mathbf{v}(s)$ is given by (ref. 13)

$$\mathbf{v}(s) = P^{-1}(s)[[P^T(-s)]^{-1}\mathbf{b}(s)e^{-\tau_g s}]_+ \tag{23}$$

where $P(s)$ is a factored matrix of $A(s)$, such that $P(s)$, as well as $P^{-1}(s)$, is analytical in the RH s-plane. Contrary to the apparent simplicity of equation (23), it is not easy to find the factored form $P(s)$ except when only a single controller is assumed. Here, $A(s)$, and hence $P(s)$ and $\mathbf{v}(s)$, degenerate into a scalar rational polynomial. The case of a single controller is summarized in appendix B.

An alternate method of finding $\mathbf{v}(s)$, including the case with $\tau_g > 0$, is summarized in appendix C. As derived there, the equivalent optimal control $\mathbf{v}(s)$ can be decomposed into two parts,

$$\mathbf{v}(s) = \mathbf{v}_o(s)e^{-\tau_g s} + \mathbf{v}_p(s;\tau_g) \tag{24}$$

where $\mathbf{v}_o(s)$ is the basic part of $\mathbf{v}(s)$ when $\tau_g = 0$, and $\mathbf{v}_p(s;\tau_g)$ is the additional part when $\tau_g > 0$.

To study the properties of $\mathbf{v}(s)$, let us consider the poles of the system with feed-forward loop closed. The fundamental characteristics of the system are governed by a set of system poles $s = -s_{uk}$; $k = 1, \ldots, k_u$, which are LH zeroes of $det[A(s)]$, that is, with $Re(s_{uk}) > 0$,

$$det[A(-s_{uk})] = 0 \; ; \qquad k = 1, \ldots, k_u \tag{25}$$

With a scalar output variable and with the first-order control surface dynamics, the number of system poles is given by

$$k_u = i_a + (\text{number of controllers}) \tag{26}$$

where i_a is the order of the least common denominator of $\mathbf{f}(s)$. Since $A(s)$ is Hermitian, equation (25) indicates that $s = s_{uk}$; $k = 1, \ldots, k_u$, is also a zero of $det[A(s)]$. Let us define a polynomial

$$d_u(s) \triangleq \prod_{k=1}^{k_u} (s + s_{uk}) \tag{27}$$

for later use. Poles s_{uk} are neither dependent on the nature of the disturbance nor on τ_g, but are dependent on the prescribed values of cost via multipliers $\mu_{f/e}$ and $\lambda_{f/e}$. Some pertinent properties of $\mathbf{v}_o(s)$ and $\mathbf{v}_p(s;\tau_g)$ will follow.

Basic Part $\mathbf{v}_o(s)$

From equation (C28a),

$$\mathbf{v}_o(s) = C^{-1}(s) \frac{\mathbf{p}_{on}(s)}{(s + \omega_g)^2 \cdot d_u(s)} \tag{28}$$

where the numerator polynomial $\mathbf{p}_{on}(s)$ is at least two orders less than that of $(s + \omega_g)^2 \cdot d_u(s)$, so that $\mathbf{v}_o(s)$ is strictly proper. This part represents the equivalent optimal control when the gust sensor is located at the CG, or equivalently $\tau_g = 0$, and is invariant whatever $\tau_g(\geq 0)$ is. The corresponding part $\mathbf{k}_o(s)$ of optimal filter $\mathbf{k}(s)$ is given by

$$\mathbf{k}_o(s) = C^{-1}(s) \frac{\mathbf{p}_{on}(s)}{(s + \omega_g)^2 d_u(s)} w_{ge}^{-1}(s) \tag{29}$$

$$= \mathbf{c}_o + \frac{\mathbf{c}_w}{s + \frac{\omega_g}{\sqrt{3}}} + \sum_{k=1}^{k_u} \frac{\mathbf{c}_k}{s + s_{uk}} \tag{29a}$$

Equation (29a) is the partial fraction form of equation (29) after extracting its constant part $\mathbf{c}_o$. Equation (29a) indicates that $\mathbf{k}_o(s)$ is composed of a train of first-order (including $\mathbf{c}_o$ term) and second-order (for complex conjugate s_{uk}) low-pass filters. Each gain $\mathbf{c}_o$, $\mathbf{c}_w$, and $\mathbf{c}_k$ has been so determined that the best compromise between performance and costs results. Figure 2a shows schematically the structure of $\mathbf{k}_o(s)e^{-\tau_g s}$, in the corresponding impulsive response function $\mathcal{L}^{-1}[\mathbf{k}_o(s)e^{-\tau_g s}]$ representation. Each element of filter $\mathbf{k}_o(s)e^{-\tau_g s}$ has an impulsive response that vanishes when $\tau < \tau_g$ for $\tau_g > 0$.

The corresponding system transfer function $g_{uo}(s) = y_o(s)/w_g(s)$ with the feed-forward loop closed is given by (see eq. (C33))

$$g_{uo}(s) = \frac{g_{uon}(s)}{\left(s + \frac{\omega_g}{\sqrt{3}}\right) \cdot d_u(s)} \tag{30}$$

where the order of $g_{uon}(s)$ is equal to that of $(s + \omega_g/\sqrt{3}) \cdot d_u(s)$ when $\mu_f \cdot \mu_e \neq 0$.

Additional Part $\mathbf{v}_p(s;\tau_g)$

The part $\mathbf{v}_p(s;\tau_g)$ is that part of $\mathbf{v}(s)$ which makes maximum utilization of the information about the turbulence that has passed the wind sensor station but has not yet reached the CG. From equation (C28b), this part is best expressed by

$$\mathbf{v}_p(s;\tau_g) = C^{-1}(s)\sum_{k=1}^{k_u}\left[\beta_{ok}\frac{e^{-\tau_g s} - e^{-\tau_g s_{uk}}}{-s + s_{uk}} + \frac{\boldsymbol{\gamma}_{pk}(0)e^{-\tau_g s} - \boldsymbol{\gamma}_{pk}(\tau_g)}{s + s_{uk}}\right] \tag{31}$$

where $\gamma_{pk}(\tau_g)$ are the coefficients dependent on τ_g and where $\gamma_{pk}(0) = \gamma_{pk}(\tau_g = 0)$. The coefficients β_{ok} are invariant with τ_g. Obviously, $\mathbf{v}_p(s;\tau_g)$, and hence the corresponding part $\mathbf{k}_p(s;\tau_g)$, are not a finite order system. This is so because of the lag ($e^{-\tau_g s}$) terms that are present in equation (31). Some consideration of a rational polynomial approximation is contained in a later section. Also, clearly $\mathbf{v}_p(s;\tau_g)$ tends to vanish when $\tau_g \to 0$, thus leaving only the $\mathbf{v}_o(s)$ portion of equation (24). It must be noted that $\mathbf{v}_p(s;\tau_g)$ is finite and analytic in the RH s-plane, even at $s = s_{uk}$; $k = 1, \ldots, k_u$. The counterpart $\mathbf{k}_p(s;\tau_g)$ of $\mathbf{k}(s)$ is written as

$$\mathbf{k}_p(s;\tau_g) = C^{-1}(s)[C(s)\mathbf{v}_p(s;\tau_g)]w_{g_e}^{-1}(s) \tag{32}$$

$$= \sum_{k=1}^{k_u}\left\{[\boldsymbol{l}_k(0)e^{-\tau_g s} - \boldsymbol{l}_k(\tau_g)] + \mathbf{r}_k\frac{e^{-\tau_g s} - e^{-\tau_g s_{uk}}}{-s + s_{uk}} + \frac{\mathbf{t}_k(0)e^{-\tau_g s} - \mathbf{t}_k(\tau_g)}{s + \omega_g/\sqrt{3}} + \frac{\mathbf{s}_k(0)e^{-\tau_g s} - \mathbf{s}_k(\tau_g)}{s + s_{uk}}\right\} \tag{32a}$$

where gain vectors $\boldsymbol{l}_k(\tau_g)$, $\mathbf{r}_k$, $\mathbf{t}_k(\tau_g)$ and $\mathbf{s}_k(\tau_g)$ are readily obtained as linear combinations of β_{ok} and $\gamma_{pk}(\tau_g)$ in equation (31). (See eq. (C37) for details.) Thus, $\mathbf{k}_p(s;\tau_g)$ as seen in (32a) constitutes another train of linear filters. Figure 2b depicts the impulse response of each term of equation (32a). As seen, the impulse responses vanish for $\tau < 0$, and hence $\mathbf{k}_p(s;\tau_g)$ is again causal. For $\tau > \tau_g$, $\mathbf{k}_p(s;\tau_g)$ is exponentially stable.

Optimal Performance and Costs

As a result of the above, one has the optimal filter of the form

$$\mathbf{k}(s) = \mathbf{k}_o(s)e^{-\tau_g s} + \mathbf{k}_p(s;\tau_g) \tag{33}$$

When equation (33) is substituted into equations (16a) and (16b) using equation (14), the performance J_y and costs $J_{uf/e}$, which are optimal in the stated sense, are obtained. Integrals in equations (16a) and (16b) are evaluated by summing up all residues in the LH or RH s-plane. The resulting J_y and $J_{uf/e}$ are implicitly dependent upon the assumed value of the multipliers $\lambda_{f/e}$ and the actuator time constants $\mu_{f/e}$ (see eq. (11)). One can then see the best trade-off between available performance and required costs with the μ and λ as parameters.

Suboptimal Filter $\tilde{\mathbf{k}}(s)$

In physical implementation of equation (33), some difficulties may arise, especially in the $\mathbf{r}_k$-terms in equation (32a). To cope with these difficulties, a rational polynomial approximation of $\mathbf{k}(s)$ seems preferable. A simple way to do this is to approximate the $e^{-\tau_g s}$ terms, as well as the $e^{-\tau_g s_{uk}}$ terms by a Padé expansion (ref. 14). It is expected that the higher the order of the polynomial approximation, the better the approximation will be (ref. 15). Just for simplicity, the first-order expansion formula

$$e^{-z} \doteq \frac{-z + a}{z + a} ; \qquad z : \text{complex} \tag{34}$$

is assumed hereinafter, with a real and positive constant a. Substituting $e^{-\tau_g s} = (-s + a/\tau_g)/(s + a/\tau_g)$ etc. into equation (33) and executing the necessary manipulations, one obtains a suboptimal filter of the form

$$\tilde{\mathbf{k}}(s) = \mathbf{k}_o(s) \frac{-s + \dfrac{a}{\tau_g}}{s + \dfrac{a}{\tau_g}} + \tilde{\mathbf{k}}_p(s;\tau_g) \tag{35}$$

where $\mathbf{k}_o(s)$ is given by equation (29a) and where

$$\tilde{\mathbf{k}}_p(s;\tau_g) = \tilde{\boldsymbol{l}}(\tau_g) + \frac{\tilde{\mathbf{r}}(\tau_g)}{s + \dfrac{a}{\tau_g}} + \frac{\tilde{\mathbf{t}}(\tau_g)}{s + \dfrac{\omega_g}{\sqrt{3}}} + \sum_{k=1}^{k_u} \frac{\tilde{\mathbf{s}}_k(\tau_g)}{s + s_{uk}} \tag{36}$$

The gain vectors $\tilde{\boldsymbol{l}}(\tau_g)$, $\tilde{\mathbf{r}}(\tau_g)$, $\tilde{\mathbf{t}}(\tau_g)$ and $\tilde{\mathbf{s}}_k(\tau_g)$ are uniquely determined as a linear combination of β_{ok} and $\tilde{\gamma}_{pk}(\tau_g)$, where $\tilde{\gamma}_{pk}(\tau_g)$ stands for the $\gamma_{pk}(\tau_g)$ which is solved with the Padé expansion of equation (34) in equations (C25b) and (C25c). It is not difficult to see that the suboptimal filter $\tilde{\mathbf{k}}(s)$ is the optimal filter of the W-H equation (eq. (21)) to which the same Padé expansion has been incorporated at the beginning. Corresponding suboptimal performance $\tilde{J}_y$ and suboptimal costs $\tilde{J}_{uf/e}$ are obtained by equations (16a) and (16b) as before.

NUMERICAL EXAMPLE AND DISCUSSION

A typical light wing-loading STOL plane is chosen in this example. The pertinent numerical data are summarized in table 1. Since we are studying the nature of the optimal filter and the resulting gust alleviation, both with and without lead time τ_g, only one flight condition (U = 41.45 m/sec) and one turbulence scale length (L = 305 m) are assumed. The necessary aerodynamic derivatives are summarized in table 2. The normal acceleration factor n_z at three fuselage stations (l_c = -2.5 m, 0.0 m, and 2.5 m correspond approximately to the cockpit, CG, and aft cabin stations, respectively) is taken as the output variable $y(s)$ (see fig. 1(a)). However, primary interest is placed on the aft cabin because it is at this station that alleviation is usually the most difficult to achieve.

TABLE 1.- AIRPLANE DATA AND FLIGHT CONDITION

Mass, kg	4,987
Wing area, m^2	39.02
Mean aerodynamic chord, m	1.981
Radius of gyration about pitch axis, m	2.576
Tail moment arm, m	7.81
True airspeed, m/sec	41.15
Altitude, m	0
Turbulence scale, m	304.8
Flap setting, deg	20

TABLE 2.- AERODYNAMIC DERIVATIVES[a]

$$\frac{\varepsilon_{\delta_f}}{\varepsilon_\alpha} = 0.465$$

Derivatives	C_T	C_D	C_L	C_m
---	0.12	0.12	0.1214	---
$\partial(\ )/\partial u$	-0.012	---	---	---
$\partial(\ )/\partial\alpha$	---	0.521	6.42	-1.26
$\partial(\ )/\partial\delta_f$	---	0.344	2.58	-0.195
$\partial(\ )/\partial\delta_e$	---	---	0.453	-1.78
$\partial(\ )/\partial\left(\frac{\dot{\alpha}c}{2U}\right)$	---	---	---	-7.97
$\partial(\ )/\partial\left(\frac{\dot{\theta}c}{2U}\right)$	---	---	---	-23.95

[a]Definitions of nondimensional derivatives in table 2 and of stability derivatives in appendix A are found in reference 18, where a conversion $w = U\alpha$ is used.

Flap Control With $\tau_g = 0$

Figure 3 shows optimal trade-off characteristics between $\sqrt{\overline{n_z^2}}/\sigma_g$ and $\sqrt{\overline{u_f^2}}/\sigma_g$ when $\tau_g = 0$ with the flap actuating system time constant $1/\mu_f$ as a parameter. As is known, a flap system (or any equivalent direct-lift controller) is very effective in alleviating the response to vertical gusts when a reasonably quick response (or large μ_f) and enough power (or large $\sqrt{\overline{u_f^2}}$) are available in the flap actuating system. When the available rms input power $\sqrt{\overline{u_f^2}}$ increases (i.e., λ_f^2 decreases), the corresponding system poles ($s = -s_{uk}$) move as shown in figure 4. Ignoring one real pole, which corresponds to an artificially introduced downwash lag pole, two pairs of complex conjugate poles modify the basic short period and phugoid poles. Another real pole modifies the surface actuating system pole ($s = -\mu_f$).

In this particular example, and in most cases with a well designed direct-lift controller, the δ_f-into-n_z transfer function $f(s)$ has only LH zeroes. Hence, considering a limiting case $\lambda_f^2 \to 0$ (with $\lambda_e^2 \to \infty$), the system poles approach the open-loop zeroes (see eq. (B11)), and an optimal control law

$$\frac{\delta_f(s)}{w_g(s)} = -\frac{g_n(s)}{f_n(s)} \tag{37}$$

is obtained (see eq. (B13)). Equation (37) defines a stable filter which could perfectly cancel the disturbance (see eq. (B14)) with a finite $\sqrt{\overline{u_f}^2}$ when $\mu_f \to \infty$, or with an infinite $\sqrt{\overline{u_f}^2}$ when $\mu_f < \infty$.

Practically, finite values of μ_f and $\sqrt{\overline{u_f}^2}$ must be considered. As seen in figure 3, a larger time constant $1/\mu_f$ requires more rms input power $\sqrt{\overline{u_f}^2}$ to achieve a given performance. The same may be seen from a different point of view in figure 5 (curve for $\tau_g = 0$) where the trade-off characteristics between $\sqrt{\overline{\delta_f}^2}$ and $\sqrt{\overline{\dot{\delta}_f}^2}$, which are required to achieve $\sqrt{\overline{n_z}^2} = 0.03$ g at the cabin station when $\sigma_g = 2.1$ m/sec, are shown. Figure 6 shows the system transfer function $g_{uo}(s)$ with the feed-forward loop closed, corresponding to several combinations of $\sqrt{\overline{\delta_f}^2}$ and $\sqrt{\overline{\dot{\delta}_f}^2}$ in figure 5. From figure 6, one can see the frequency-wise structure of the achieved alleviation. As seen, a smaller time constant $1/\mu_f$ provides more alleviation at the high frequencies, but less alleviation at the low frequencies. Figures 5 and 6 clearly show that a clever choice must be made from the ride-qualities standpoint to achieve a proper compromise between the frequency band to be alleviated and the available $\sqrt{\overline{\delta_f}^2}$ and $\sqrt{\overline{\dot{\delta}_f}^2}$.

Flap Control With $\tau_g > 0$

As indicated in appendix B (see eq. (B13)), lead time $\tau_g(>0)$ is unnecessary when enough $\sqrt{\overline{u_f}^2}$ is available. In other words, if the flap surface can be actuated quickly enough and the effect thereof is of minimum phase lag, then the corrective control need not be initiated before the disturbance arrives. When $\sqrt{\overline{u_f^2}}$ is finite however, lead time τ_g reduces the required cost to some extent. Examples are shown in figure 7. Although it is unrealistic, the limiting case $\tau_g \to \infty$ is included to indicate how lead time τ_g affects gust alleviation. When $1/\mu_f$ is zero (fig. 7(a)), only a negligible cost saving is available with a realistic value of $\tau_g = 0.1$ sec. When $1/\mu_f$ is 0.5 sec (fig. 7(b)) some improvement is realized by small lead values ($\tau_g = 0.1$ sec). These cost savings are also compared in figure 5 with $1/\mu_f$ and τ_g as parameters.

Generally, the merit of lead time τ_g is only realized when the actuating system response is slow. This fact would be further emphasized when a sub-optimal filter is substituted for the optimal one. The broken lines in figure 7 show the performance corresponding to a rational polynomial filter as given by equation (35) with $a = 2$. In these examples, apparently the disadvantage introduced by rational polynomial approximation destroys the merit of positive τ_g. This shows that a higher-order Padé approximation would be necessary.

Elevator Control With $\tau_g = 0$

Figure 8 shows the optimal trade-off between $\sqrt{\overline{n_z^2}}/\sigma_g$ and $\sqrt{\overline{u_e^2}}/\sigma_g$ with $\tau_g = 0$ at the three fuselage stations. As is well known, the elevator is not an effective gust alleviator, especially at the aft cabin station. This is due to non-minimum phase lag characteristics of the δ_e-into-n_z transfer function $e(s)$. Figure 9 shows the system poles $s = -s_{uk}$ with $\sqrt{\overline{u_e^2}}$ (or equivalently with λ_e^2) as a parameter at the cabin station. When allowable $\sqrt{\overline{u_e^2}}$ increases, similar to the flap case, system poles start from open loop poles and approach the zeroes of $e(s)$. When there is a non-minimum phase zero, such as shown in figure 9, one of the system poles corresponding to the short period mode terminates at the image in the LH s-plane of the RH zero. This is what is indicated in equation (B16). The limiting case $\lambda_e^2 \to 0$ (with $\lambda_f^2 \to \infty$) gives an optimal control law (see eq. (B18))

$$\frac{\delta_e(s)}{w_g(s)} = -\frac{1}{c_{g_e}} \cdot \frac{g_n^*(s)}{e_n^*(s)\left(s + \frac{\omega_g}{\sqrt{3}}\right)} \tag{38}$$

where $e_n^*(s)$ is $e_n(s)$ with replacement of its RH zero factor $(-s + z_e)$ by its image factor $(s + z_e)$, and where $g_n^*(s)$ is a polynomial defined by equation (B20). Equation (38) defines another stable filter, but, in this case, perfect alleviation is not obtained. In fact, the corresponding system response is given by (see eq. (B21))

$$g_{uo}(s) = \frac{\rho_e}{c_{g_e}} \cdot \frac{(s + \omega_g)^2}{\left(s + \frac{\omega_g}{\sqrt{3}}\right) \cdot (s + z_e)} = \frac{\rho_e}{s + z_e} w_{g_e}^{-1}(s) \tag{39}$$

where

$$\rho_e = 2z_e g(z_e) w_{g_e}(z_e) \tag{40}$$

In figure 10, which shows system response $g_{uo}(s)$ with λ_e as a parameter, one can see the frequency-wise structure of the alleviation. It is clear from the figure that the desired alleviation in rms $\sqrt{\bar{n}_z^2}$ is obtained only at the sacrifice of amplified response in the low- and high-frequency ranges. Finally, the best available performance corresponding to the limiting case $\lambda_e^2 \to 0$ is obtained from equations (16a) and (39),

$$\left(\sqrt{\bar{n}_z^2}\right)_o = \sqrt{\frac{\pi}{2}} \cdot \frac{\rho_e}{\sqrt{z_e}} \tag{41}$$

which is achieved with infinite cost $\sqrt{\bar{u}_e^2}$. Using equations (40) and (19a), equation (41) is rewritten in a more practical form:

$$\left(\frac{\sqrt{\bar{n}_z^2}}{\sigma_g}\right)_o = \sqrt{6\omega_g z_e} \cdot \frac{z_e + \omega_g/\sqrt{3}}{(z_e + \omega_g)^2} \cdot g(z_e) \tag{41a}$$

The inefficiency of elevator control as a gust alleviator depends on the fuselage station because the location of the RH zero $s = z_e$ is dependent upon the station as well as on the flight conditions. The limiting performance of equation (41) without lead time in gust sensing is plotted in the $\tau_g = 0$ curve in figure 11 against fuselage station. At the fuselage station aft of the center of percussion ($l_c > l_{cc}$, l_{cc} is positive rearward from CG), the ride quality becomes worse. At the stations before l_{cc}, there exist no RH zeroes in $e_n(s)$, hence theoretically perfect alleviation is achievable with enough input power $\sqrt{\bar{u}_e^2}$ as in the case of flap control. Using the short period mode approximation, the marginal point l_{cc} (center of percussion) is given by

$$\frac{l_{cc}}{c} = -\left(\frac{k_y}{c}\right)^2 \cdot \frac{C_{z_{\delta_e}}}{C_{m_{\delta_e}}} \tag{42}$$

Elevator Control With $\tau_g > 0$

Let us consider the same limiting performance when $\lambda_e^2 \to 0$ with $\tau_g > 0$ at fuselage stations $l_c > l_{cc}$. As derived in appendix B, the additional part of the filter adds the corrective control

$$\frac{\delta_e(s)}{w_g(s)} = -\rho_e \frac{d_\alpha(s)}{e_n^*(s)} \cdot \frac{e^{-\tau_g s} - e^{-\tau_g z_e}}{-s + z_e} w_{g_e}^{-1}(s) e^{\tau_g s} \tag{43}$$

and this results in a total system response (see eq. (B23)) of

$$g_u(s) = g_{uo}(s) e^{-\tau_g z_e} e^{\tau_g s} \tag{44}$$

and the limiting performance as $\sqrt{\bar{u}_e^2} \to \infty$ of

$$\frac{\sqrt{\bar{n}_z^2}}{\sigma_g} = \left(\frac{\sqrt{\bar{n}_z^2}}{\sigma_g}\right)_o \cdot e^{-\tau_g z_e} \tag{45}$$

Although equations (44) and (45) are only realized with an infinite control input $\sqrt{\bar{u}_e^2}$, they suggest the possible improvement that lead time τ_g gives, an improvement that can be significant especially when z_e is large. The essential role of $\delta_e(s)/w_g(s)$ in equation (43) is that the RH zero in $e(s)$ is cancelled out by the same factor in the filter denominator when $g_{up}(s)$ is considered (see eq. (B22)). However, when a finite cost $\sqrt{\bar{u}_e^2}$ (with $\lambda_e^2 > 0$) is prescribed, such a pole-zero cancellation occurs only partially. The effect of the additional part of the filter is shown in figure 11 with $\tau_g > 0$ as a parameter. Figures 12(a) through (c) show the optimal trade-off between $\sqrt{\bar{n}_z^2}/\sigma_g$ and $\sqrt{\bar{u}_e^2}/\sigma_g$ when $\tau_g > 0$ at the three fuselage stations. The ride improvement is considerable when $\tau_g \geq 0.1$ sec at the aft cabin. As is predicted by equation (44), the alleviation due to a filter which includes the additional lead time part covers a wide frequency band. This is shown in figure 13 where system response $g_u(s)$ with and without lead time is compared.

The performance with suboptimal filters as given by equation (35) shows no significant performance degradation with $a = 2$. This suboptimal filter is compared with the optimal filter in figure 13 for the case of $\lambda_e = 0.1$ and $\tau_g = 0.1$ sec.

Two Controllers

It has been shown that the flap control is effective for gust alleviation, if enough control power is provided, and that the effectiveness of elevator control as a gust suppressor is improved by feeding the disturbance signal in with lead time. Now let us consider how much the required flap system cost could be reduced by incorporating the elevator as an auxiliary controller. Figures 14(a) and 14(b) show optimal trade-off characteristics between $\sqrt{\bar{n}_z^2}/\sigma_g$, $\sqrt{\bar{u}_f^2}/\sigma_g$, and $\sqrt{\bar{u}_e^2}/\sigma_g$ with τ_g as a parameter. These figures are results of the exact filter of equation (33), but the results using the suboptimal filter of equation (35) with $a = 2$ differ only indiscernibly from those shown. This is not true for much higher $\sqrt{\bar{u}_f^2}$ than shown or for the cases with smaller time constant $1/\mu_f$. (See suboptimal performance in figs. 7(a) and 7(b).) Similar to the single controller case, the elevator shows some effectiveness at the cockpit station even when $\tau_g = 0$, but it makes little contribution at the aft cabin station. When $\tau_g > 0$, the situation is improved considerably at the cabin station.

Hereinafter, attention will be focused on the aft cabin station, where non-minimum phase lag characteristics hamper the effectiveness of elevator control. The cost savings achieved in the flap system by incorporating the elevator, is shown in figure 15. In the figure, required costs $\sqrt{\bar{\delta}_f^2}$ and $\sqrt{\bar{\dot{\delta}}_f^2}$ to obtain $\sqrt{\bar{n}_z^2} = 0.03$ g for $\sigma_g = 2.1$ m/sec are plotted with rms elevator power $\sqrt{\bar{u}_e^2}$ and flap time constant $1/\mu_f$ as parameters for $\tau_g = 0$ sec and 0.1 sec. These results are based upon the use of a suboptimal filter as in equation (35), and hence the adverse effects of rational polynomial approximation appear when $1/\mu_f$ is small with $\tau_g > 0$. Except for this fact, it is seen that much greater cost savings can be achieved in the flap system by elevator control when $\tau_g > 0$. As to the frequency-wise structure of the alleviated system, several cases are compared in figure 16 in their system transfer function $g_u(s)$. The figure indicates that the resulting alleviation by two controllers is the blended one of the single controller cases of figures 6 and 13. This is shown by the fact that the corresponding system poles $s = -s_{uk}$ are located between the optimal pole locations in the single controller cases. This is seen in figure 17 where the system poles corresponding to the short period mode are shown. Locations of the other poles are almost the same as those in the single controller cases.

Limiting Cases

As has been seen in the above, if one is concerned with a given criteria such as $\sqrt{\bar{n}_z^2}/\sigma_g = 0.03$ g/2.1 m/sec at a particular fuselage station, there is a family of required costs $(\mu_f, \sqrt{\bar{u}_f^2})$ and $(\mu_e, \sqrt{\bar{u}_e^2})$, or equivalently $(\sqrt{\bar{\delta}_f^2}, \sqrt{\bar{\dot{\delta}}_f^2})$ and $(\sqrt{\bar{\delta}_e^2}, \sqrt{\bar{\dot{\delta}}_e^2})$, as illustrated in figure 18. To obtain a rough idea of system performance, including the power spectrum characteristics and required costs, two limiting cases are considered. One is the case of flaps only $(\lambda_e^2 \to \infty)$; it corresponds to point F in figure 18 and has been described before. The other is the case assuming an infinite elevator control. It is indicated by point E in figure 18 and is characterized by $\lambda_e^2 \to 0$ while retaining λ_f^2 finite. A process similar to the one used in appendix B (limiting case $\lambda^2 \to 0$) leads to somewhat simple formulas. Inspection of equation (C16) gives the limiting characteristics

$$\nu d_u(s) \to \lambda_f \frac{s + c_\infty}{c_\infty} \cdot \frac{s + \mu_f}{\mu_f} e_n{}^*(s) \; ; \qquad c_\infty = \frac{\mu_e}{\lambda_e} e_{no} \tag{46}$$

where e_{no} is the leading term coefficient of $e_n(s)$ and where $e_n{}^*(s)$ has the same definition that is used in equation (38). Also, equation (C19) yields

$$A^{-1}(s)\mathbf{b}(s) \to \begin{bmatrix} 0 \\ \dfrac{s+\mu_e}{\mu_e} \cdot \dfrac{c_\infty}{-s+c_\infty} \cdot \dfrac{c_\infty}{s+c_\infty} \cdot \dfrac{g_n(s)}{e_n(s)} \cdot w_{g_e}(s) \end{bmatrix} \tag{47}$$

Denoting by $v^f(s)$ and $v^e(s)$, and $\rho^f(s)$ and $\rho^e(s)$ the flap and elevator components of $\mathbf{v}(s)$ and $\boldsymbol{\rho}(s)$, respectively, equation (47) indicates (see eq. (C9))

$$v^f(s) = -\frac{s+\mu_f}{\mu_f}\,\rho^f(s) \tag{48a}$$

$$v^e(s) = \frac{s+\mu_e}{\mu_e}\left[\frac{c_\infty}{-s+c_\infty} \cdot \frac{c_\infty}{s+c_\infty} \cdot \frac{g_n(s)}{e_n(s)}\, w_{g_e}(s) e^{-\tau_g s} - \rho^e(s)\right] \tag{48b}$$

In equation (48a), $\rho^f(s)$ has no poles other than $d_u(s)$ zeroes, which comprise the LH zeroes of $e_n{}^*(s)$ as well as $s = -\mu_f$ and $s = -c_\infty$. Evaluating equation (C25a) at these poles, it can be shown that all the unknown coefficients in $\rho^f(s)$ vanish except for the ones, $\gamma^f_{p\mu}(\tau_g)$ and $\gamma^f_{pe}(\tau_g)$, which are the gains corresponding to the poles $s = -\mu_f$ and $s = -z_e$, respectively. Further, equation (C25c) requires $\gamma^f_{p\mu}(\tau_g) + \gamma^f_{pe}(\tau_g) = 0$, so that one can write

$$\begin{aligned} \rho^f(s) &= \frac{\gamma^f_{p\mu}(\tau_g)}{s+\mu_f} + \frac{\gamma^f_{pe}(\tau_g)}{s+z_e} \\ &= \frac{(\mu_f - z_e)\gamma^f_{pe}(\tau_g)}{(s+\mu_f)(s+z_e)} \end{aligned} \tag{49}$$

Now considering equation (47) again, the only possible RH pole in $\rho^e(s)$ is $s = z_e$, which comes out of $e_n(s)$. This implies that the RH members of equations (C25b) and (C25c) are proportional to $e^{-\tau_g z_e}$, and hence that all the unknown coefficients $\gamma^f_p(\tau_g)$ and $\gamma^e_p(\tau_g)$ are given by $\gamma^f_p(0) \cdot e^{-\tau_g z_e}$ and $\gamma^e_p(0) e^{-\tau_g z_e}$, respectively. Thus, substituting equation (49) into equation (48a), one has

$$v^f(s) = -\frac{\mu_f - z_e}{\mu_f} \cdot \frac{\gamma^f_{pe}(0)}{s+z_e}\, e^{-\tau_g z_e} \tag{50}$$

which gives the required cost in the flap system

$$\sqrt{\bar{u}_f^2} = \sqrt{\frac{\pi}{2z_e}} \cdot \left| \frac{\mu_f - z_e}{\mu_f} \gamma_{pe}^f(0) \right| \cdot e^{-\tau_g z_e} \tag{51}$$

The elevator component $v^e(s)$ has a similar structure to that of equation (B18), except that it includes an additional pole $s = -\mu_f$, and that both $g_n{}^*(s)$ and ρ_e are now dependent upon $\lambda_f{}^2$. The corresponding system transfer function of equation (14) is written as

$$g_u(s) = g(s) - [f(s)e(s)]C(s) \begin{bmatrix} v^f(s) \\ v^e(s) \end{bmatrix} w_{g_e}^{-1}(s) e^{\tau_g s} \tag{52}$$

Substitution of equations (48a) and (48b) into equation (52) gives a limit when $c_\infty \to \infty$

$$g_u(s) \to \left[f(s)\rho^f(s) + e(s)\rho^e(s) \right] w_{g_e}^{-1}(s) e^{\tau_g s} \tag{53}$$

Taking the requirements of equations (C25a) through (C25c) into account, one can expand the RH [ ] of equation (53) into partial fractions and find that

$$g_u(s) = \frac{\rho_{ef}}{s + z_e} w_{g_e}^{-1}(s) e^{-\tau_g z_e} e^{\tau_g s} \tag{54}$$

where the system gain ρ_{ef} is given by

$$\rho_{ef} = \frac{\lambda_f{}^2}{\mu_f{}^2} \cdot \frac{z_e{}^2 - \mu_f{}^2}{f(z_e)} \gamma_{pe}^f(0) \tag{55}$$

Equation (54), a very similar expression to equation (44), which is the limiting case of elevator control, indicates that the output $y(s) = n_z(s)$ has a power spectrum

$$\Phi_{n_z}(\omega) = \frac{\rho_{ef}^2}{\omega^2 + z_e{}^2} e^{-2\tau_g z_e} \tag{56}$$

which is to be compared with the output power spectrum of open loop

$$[\Phi_{n_z}(\omega)]_o = g(-j\omega)\Phi_{w_g}(\omega)g(j\omega) \tag{57}$$

Finally, equation (56) gives a limiting performance

$$\sqrt{\bar{n}_z{}^2} = \sqrt{\frac{\pi}{2}} \cdot \frac{|\rho_{ef}|}{\sqrt{z_e}} \cdot e^{-\tau_g z_e} \tag{58}$$

Since the filter gain $\gamma_{pe}^{f}(0)$, and hence the system gain ρ_{ef}, is implicitly dependent on the assumed value of λ_f as well as on μ_f, equations (51) and (58) do not afford a pair of closed form solutions of the flap cost and performance. However, it may be noted that the algorithm required to solve for the unknown gains is greatly simplified in this limiting case.

An example of the reduction in the flap cost available by incorporating elevator control to achieve a given performance has been shown in figure 15. It is seen in figure 15 that a much greater cost reduction is realized in the flap system when the elevator control is used together with a positive lead time (e.g., τ_g = 0.1 sec) than when it is used without lead time (τ_g = 0 sec). Figure 19 compares the output power spectra corresponding to $\sqrt{\bar{u}_e{}^2} = 0$ (point F) and to $\sqrt{\bar{u}_e{}^2} \to \infty$ (point E) with that of open loop. When the loop is open, two peaks appear in $[\Phi_{n_z}(\omega)]_o$ corresponding to the phugoid and the short period modes. The turbulence spectrum $\Phi_{w_g}(\omega)$ and the transfer function $g(s)$ cut off the output spectrum at the high- and low-frequency ranges, respectively. The same feature exists in the flap case (point F) where optimally relocated poles and zeroes result in a gust alleviation. In the two controller case (point E), the infinite elevator cost eliminates all the inherent poles and zeroes except one image pole $s = -z_e$. Thus the output spectrum $\Phi_{n_z}(\omega)$ is not attenuated in its low frequency range.

CONCLUSIONS

An analytical study was made of an optimal gust alleviation system that uses vertical gust sensors mounted ahead of the CG. Frequency domain optimization techniques were used to synthesize the optimal filters that produce the corrective control signals into the flap and elevator actuators. A special emphasis was placed upon the effectiveness of the time by which sensor information leads the actual encounter of the gust in reducing the rms value of vertical acceleration caused by the gust. The resulting filter, a lagging filter when the lead time is positive, is expressed as an implicit function of the prescribed control costs; that is, prescribed rms values of surface deflection and its time rate. Using this method, the optimal trade-off between system performance and required costs was systematically studied. A numerical example, which considers a light wing-loading airplane in the approach condition, is included. The conclusions derived from the study are that optimal feed-forward of gust signal with positive lead time results in the following.

1. It improves the cost-effectiveness of flap control, especially when the flap actuating system has a large time constant.

2. It improves cost-effectiveness of the elevator control significantly, especially at the aft cabin stations where otherwise non-minimum phase lag

characteristics hamper the elevator's effectiveness. Elevator control both with and without flap control decreases the rms vertical acceleration by a factor $e^{-\tau_g z_e}$ times that with the zero lead time $\tau_g = 0$ case, if enough elevator control power is available.

Ames Research Center
National Aeronautics and Space Administration
Moffett Field, California 94035, August 19, 1975

APPENDIX A

STATE EQUATIONS

The longitudinal equations of motion defining the response of an aircraft to control inputs and disturbance are written as

$$\begin{bmatrix} s - X_u & -X_\alpha & g \\ -Z_u & s - Z_\alpha & -s \\ -M_u & -(M_{\dot{\alpha}} s + M_\alpha) & s(s - M_q) \end{bmatrix} \begin{bmatrix} u(s) \\ \alpha(s) \\ \theta(s) \end{bmatrix}$$

$$= \begin{bmatrix} X_{\delta_f} & X_{\delta_e} \\ Z_{\delta_f} & Z_{\delta_e} \\ M_{\dot{\delta}_f} s + M_{\delta_f} & M_{\delta_e} \end{bmatrix} \begin{bmatrix} \delta_f(s) \\ \delta_e(s) \end{bmatrix} + \begin{bmatrix} X_u & X_\alpha / U \\ Z_u & Z_\alpha / U \\ M_u & [(M_{\dot{\alpha}} - M_q)s + M_\alpha]/U \end{bmatrix} \begin{bmatrix} u_g(s) \\ w_g(s) \end{bmatrix} \tag{A1}$$

where the linear representation of the vertical gust

$$\left.\begin{aligned} \alpha_g &= \frac{w_g}{U} \\ \dot{\alpha}_g &= \frac{1}{U} \frac{\partial w_g}{\partial t} \\ q_g &= -\frac{\partial w_g}{\partial x} = -\frac{1}{U} \frac{\partial w_g}{\partial t} \end{aligned}\right\} \tag{A2}$$

is assumed. Also assumed in equation (A1) is the first-order expansion in downwash lag terms such as

$$\alpha(t) - \alpha\left(t - \frac{l_T}{U}\right) = \frac{l_T}{U} \dot{\alpha}(t) \tag{A3a}$$

or equivalently in the frequency domain

$$\left[1 - e^{-(l_T/U)s}\right] \alpha(s) = \frac{l_T}{U} s\alpha(s) \tag{A3b}$$

Inspection of the moment equation in equation (A1) indicates that response $\ddot{\theta}$ due to δ_f or w_g, or both, becomes very high in the high frequency range. This is of no consequence in the conventional analysis of rigid body modes; however, if one is concerned with the rms value of a response evaluated over the frequency range $[0,\infty)$, this unrealistic feature must be avoided. For this reason, the first-order Padé expansion $e^{-z} = (-z + 2)/(z + 2)$ is used in this analysis so that equation (A3b) becomes

$$\left[1 - e^{-(l_T/U)s}\right]\alpha(s) = \frac{\frac{2U}{l_T}}{s + \frac{2U}{l_T}} \cdot \frac{l_T}{U}\, s\alpha(s) \tag{A4}$$

Consequently, terms $M_{\dot{\alpha}}s$, $M_{\dot{\delta}_f}s$, and $(M_{\dot{\alpha}} - M_q)s$ in equation (A1) are multiplied by the factor $(2U/l_T)/[s + (2U/l_T)]$.

By multiplying the inverse of the LH coefficient matrix in equation (A1), explicit forms of $F_\alpha(s)$ and $G_\alpha(s)$ are obtained.

APPENDIX B

THE WIENER-HOPF EQUATION AND ITS SOLUTION

Wiener-Hopf Equation

Given is an augmented performance index J (eqs. (15), (16a), and (16b),

$$J = J_y + \lambda_f^2 J_{uf} + \lambda_e^2 J_{ue}$$

$$= \frac{1}{2}\int_{-\infty}^{\infty} \{[g(j\omega)w_{g_e}(j\omega) - \mathbf{f}^T(j\omega)C(j\omega)\mathbf{v}(j\omega)e^{j\omega\tau_g}]$$

$$\times[w_{g_e}(-j\omega)g(-j\omega) - \mathbf{v}^T(-j\omega)C(-j\omega)\mathbf{f}(-j\omega)e^{-j\omega\tau_g}]$$

$$+\mathbf{v}^T(-j\omega)\Lambda\mathbf{v}(j\omega)\}d\omega \tag{B1}$$

Required is a stable and causal $\mathbf{v}(s)$ such that $\mathbf{v}(j\omega)$ minimizes J. The first variation δJ due to an infinitely small variation $\delta\mathbf{v}(j\omega)$ is given by

$$\delta J = \frac{1}{2}\int_{-\infty}^{\infty} [\delta\mathbf{v}^T(-j\omega)\mathbf{z}(j\omega) + \mathbf{z}^T(-j\omega)\delta\mathbf{v}(j\omega)]d\omega \tag{B2}$$

with

$$\mathbf{z}(j\omega) = [\Lambda + C(-j\omega)\mathbf{f}(-j\omega)\mathbf{f}^T(j\omega)C(j\omega)]\mathbf{v}(j\omega)$$

$$-C(-j\omega)\mathbf{f}(-j\omega)g(j\omega)w_{g_e}(j\omega)e^{-j\tau_g\omega} \tag{B3}$$

In order that $\delta J = 0$ for any variation $\delta\mathbf{v}(s)$, which is analytic in the RH s-plane, $\mathbf{z}(s)$ must be analytic in the LH s-plane, see, for example, reference 9; this is stated by equation (21). It must be noted that, if $\mathbf{v}(s)$ is analytic in the RH s-plane, then so is $\mathbf{k}(s)$ of equation (20) and vice versa.

Solution $\mathbf{v}(s)$

Since the matrix $A(s)$ in equation (22a) is real on the $j\omega$ axis, conjugate, and Hermitian, and has a maximum rank of 2 (when $\lambda_f^2 \cdot \lambda_e^2 \neq 0$) or 1 (when λ_f^2 or $\lambda_e^2 = 0$), there exists a (2×2) or (1×1) matrix $P(s)$ such that

$$A(s) = P^T(-s)P(s) \tag{B4}$$

and that $P(s)$ as well as its inverse $P^{-1}(s)$, is analytic in the RH s-plane (ref. 13). Hence, the solution $\mathbf{v}(s)$ is given by the closed form

$$\mathbf{v}(s) = P^{-1}(s)\left[[P^T(-s)]^{-1}\mathbf{b}(s)e^{-\tau_g s}\right]_+ \tag{B5}$$

Single Controller Case

Let $f_1(s) = f_{1n}(s)/d_a(s)$ be either $f(s)$ or $e(s)$ of equation (6), and λ and μ be corresponding multipliers. Matrix $A(s)$ and vector $\mathbf{b}(s)$ of equations (22a) and (22b) become scalars, and the factored form $P(s)$ is readily given by

$$P(s) = \frac{\nu d_u(s)}{d_c(s)d_a(s)} \tag{B6}$$

where, using a shorthand notation $d_c(s) = s + \mu$ and a real constant ν,

$$\nu^2 d_u(-s)d_u(s) = \lambda^2 d_c(-s)d_a(-s)d_a(s)d_c(s) + \mu^2 f_{1n}(-s)f_{1n}(s) \tag{B7}$$

and where $d_u(s)$ has only LH zeroes $s = -s_{uk}$; $k = 1, \ldots, k_u$; $k_u = i_a + 1$. After partial fraction expansion, the rational polynomial $[P^T(-s)]^{-1}\mathbf{b}(s)$ is expanded as follows

$$\begin{aligned}[P^T(-s)]^{-1}\mathbf{b}(s)e^{-\tau_g s} &= \frac{\mu}{\nu}\cdot\frac{f_{1n}(-s)g_n(s)}{d_u(-s)d_a(s)}\,w_{g_e}(s)e^{-\tau_g s} \\ &= \frac{\mu}{\nu}\left\{\left[\frac{f_{1n}(-s)g_n(s)}{d_u(-s)d_a(s)}w_{g_e}(s)\right]_+ + \sum_{k=1}^{k_u}\frac{\beta_k}{-s + s_{uk}}\right\}e^{-\tau_g s}\end{aligned} \tag{B8}$$

where the $[\quad\cdot\ \cdot\ \cdot\quad]_+$ term has poles of $d_a(s)$ and of $w_{g_e}(s)$. Knowing that

$$\begin{aligned}\left[\frac{e^{-\tau_g s}}{-s + s_{uk}}\right]_+ &= \int_o^\infty e^{-st}\left(\frac{1}{2\pi j}\int_{-j\infty}^{j\infty}\frac{e^{-\tau_g s}}{-s + s_{uk}}\,e^{ts}\,ds\right)dt \\ &= \frac{e^{-\tau_g s} - e^{-\tau_g s_{uk}}}{-s + s_{uk}}\end{aligned} \tag{B9}$$

the solution $v(s)$ of equation (B5) is written as

$$v(s) = \left(\frac{\mu}{\nu}\right)^2 \frac{d_c(s)}{\mu} \frac{d_a(s)}{d_u(s)} \left\{ \left[\frac{f_{1n}(-s) g_n(s)}{d_u(-s) d_a(s)} w_{g_e}(s) \right]_+ \cdot e^{-\tau_g s} + \sum_{k=1}^{k_u} \beta_k \frac{e^{-\tau_g s} - e^{-\tau_g s_{uk}}}{-s + s_{uk}} \right\} \tag{B10}$$

After another partial fraction expansion, equation (B10) is rearranged into the standard form in equations (24), (28) and (31).

Limiting Case $\lambda^2 \to 0$

A special case where an infinite cost is allowed, is specified by letting $\lambda^2 \to 0$. If $f_{1n}(s)$ has no RH zeroes, equation (B7) implies that the system poles approach either LH zeroes of $f_{1n}(s)$ or $s = -c_\infty$ when $\lambda^2 \to 0$, so that

$$\nu d_u(s) \to \mu f_{1n}(s) \frac{s + c_\infty}{c_\infty} \; ; \qquad c_\infty = \frac{\mu f_{1no}}{\lambda} \tag{B11}$$

where f_{1no} is the leading term coefficient of $f_{1n}(s)$. Equation (B8) simplifies to

$$[P^T(-s)]^{-1} \mathbf{b}(s) e^{-\tau_g s} \to \frac{c_\infty}{-s + c_\infty} \cdot \frac{g_n(s)}{d_a(s)} w_{g_e}(s) e^{-\tau_g s} \tag{B12}$$

Applying $[\ ]_+$ operator to equation (B12) while retaining λ^2 as finite and finally letting $\lambda^2 \to 0$, one can see that the contribution of $c_\infty/(-s + c_\infty)$, which is the only possibility yielding the additional part of the filter, vanishes even when $\tau_g > 0$. Hence, the limiting case without the non-minimum phase zero is obtained as follows:

$$v(s) = \frac{c_\infty}{\mu} \cdot \frac{s + \mu}{s + c_\infty} \cdot \frac{g_n(s)}{f_n(s)} w_{g_e}(s) e^{-\tau_g s} \tag{B13}$$

$$\to \frac{s + \mu}{\mu} \cdot \frac{g_n(s)}{f_n(s)} w_{g_e}(s) e^{-\tau_g s} \; ; \qquad |s| < \infty \tag{B13a}$$

which gives, in turn

$$g_u(s) \to 0 \tag{B14}$$

where $g_u(s)$ is the system response that is defined by equation (14).

Next, suppose $f_{1n}(s)$ has a RH real zero, $s = z_e$, with $z_e > 0$. Putting

$$f_{1n}(s) = (-s + z_e)f^*_{1n}(s) \tag{B15}$$

$f^*_{1n}(s)$ has LH zeroes only. This time, equation (B7) has a limit

$$\nu d_u(s) \to \mu(s + z_e)f^*_{1n}(s)\,\frac{s + c_\infty}{c_\infty} \tag{B16}$$

and hence,

$$[P^T(-s)]^{-1}\mathbf{b}(s)e^{-\tau_g s} \to \frac{c_\infty}{-s + c_\infty}\cdot\frac{s + z_e}{-s + z_e}\cdot\frac{g_n(s)}{d_a(s)}\,w_{g_e}(s)e^{-\tau_g s} \tag{B17}$$

As a result, from equation (B5), a limiting case with the non-minimum phase lag is obtained as follows:

$$v(s) \to \frac{s + \mu}{\mu}\left[\frac{g_n{}^*(s)}{(s + z_e)f^*_{1n}(s)(s + \omega_g)^2}\,e^{-\tau_g s}\right.$$

$$\left. + \rho_e\,\frac{d_a(s)}{(s + z_e)f^*_{1n}(s)}\cdot\frac{e^{-\tau_g s} - e^{-\tau_g z_e}}{-s + z_e}\right]; \qquad |s| < \infty \tag{B18}$$

where

$$\rho_e = 2z_e[g(s)w_{g_e}(s)]_{s=z_e} \tag{B19}$$

and where $g_n{}^*(s)$ is a polynomial of order k_u such that

$$(-s + z_e)g_n{}^*(s) = c_{g_e}(s + \omega_g/\sqrt{3})(s + z_e)g_n(s) - \rho_e\,d_a(s)(s + \omega_g)^2 \tag{B20}$$

Equation (B18), in contrast with equation (B13a), comprises both the basic and the additional parts of the filter. The basic part in equation (B18) gives a system response

$$g_{u_o}(s) \to g(s) - f(s)\,\frac{g_n{}^*(s)}{(s + z_e)f^*_{1n}(s)(s + \omega_g)^2}\,w^{-1}_{g_e}(s) = \frac{\rho_e}{s + z_e}\,w^{-1}_{g_e}(s) \tag{B21}$$

and the additional part in equation (B18) gives an additional response

$$g_{up}(s) \rightarrow -f(s)\rho_e \frac{d_a(s)}{(s + z_e)f_{in}^*(s)} \cdot \frac{e^{-\tau_g s} - e^{-\tau_g z_e}}{-s + z_e} w_{g_e}^{-1}(s)e^{\tau_g s} \tag{B22}$$

$$= - \frac{\rho_e}{s + z_e} (1 - e^{-\tau_g z_e} e^{\tau_g s})w_{g_e}^{-1}(s) \tag{B22a}$$

It must be noted that, in equation (B22), the factor $(-s + z_e)$ in the numerator of $f(s)$ is cancelled out by the same factor in the filter denominator. This is the essential role of the additional part of the filter. From equations (B21) and (B22a),

$$g_u(s) = g_{uo}(s) + g_{up}(s) = \frac{\rho_e}{s + z_e} e^{-\tau_g z_e} e^{\tau_g s} w_{g_e}^{-1}(s) \tag{B23}$$

is obtained for the total system response.

APPENDIX C

ALTERNATE METHOD TO SOLVE THE WIENER-HOPF EQUATION

References 16 and 17 provide practical methods of solving a given Wiener-Hopf equation without finding the explicit form of $P(s)$ when $\tau_g = 0$; however, those methods are not applicable when $\tau_g > 0$. The following is an extension to include such a case.

Preliminary 1

Let $h(s)$ be a scalar rational polynomial which is strictly proper,[1]

$$h(s) = \frac{q(s)}{r(-s) \cdot l(s)} \tag{C1}$$

where $r(-s) = \prod_i (-s + s_{r_i})$ and $l(s) = \prod_k (s + s_{lk})$ with $Re(s_{r_i}, s_{lk}) > 0$, so that $s = s_{r_i}$ and $s = -s_{lk}$ are poles of $h(s)$ in the RH and LH s-planes, respectively. Denoting by $[\ ]_+$ and $[\ ]_-$ those parts of $[\ ]$ which are analytic in RH and LH s-planes, respectively. Then, when $\tau_g > 0$

$$[h(s)e^{-\tau_g s}]_+ = h(s)e^{-\tau_g s} - \zeta(s) \tag{C2}$$

where $\zeta(s)$ is a strictly proper rational polynomial in s. The reason is as follows. By Fourier's integral formula, $h(s)e^{-\tau_g s}$ is expanded into $[\ ]_+$ and $[\ ]_-$ parts, where

$$[h(s)e^{-\tau_g s}]_- = \int_{-\infty}^{0} e^{-st}\, dt \left[\frac{1}{2\pi j}\int_{-j\infty}^{j\infty} h(\sigma)e^{(t-\tau_g)\sigma}\, d\sigma\right]$$

$$= \sum_i \frac{q_{r_i}\, e^{-\tau_g s_{r_i}}}{-s + s_{r_i}} \tag{C3}$$

with unique coefficients q_{r_i}. The Σ term just above is denoted as $\zeta(s)$, which has the stated properties. Equation (C2) is valid even when s_{r_i} is a multiple pole. What is implied by equation (C2) is that, by evaluating $[\ ]_-$, which is

[1]A rational polynomial is proper when the order of the numerator polynomial is not greater than that of the denominator. If the numerator's order is less than that of denominator, the rational polynomial is strictly proper.

a rational polynomial in s, one can avoid difficulty in evaluating the $[\ ]_+$ part, which is not a simple rational polynomial, but includes $e^{-\tau_g s}$ terms.

Preliminary 2

The matrix $A(s)$ of equation (22a) may be modified as follows,

$$A(s) = C(-s)A^*(s)C(s) \tag{C4}$$

where

$$A^*(s) = \frac{d_a(-s)d_a(s)C^{-1}(-s)\Lambda C^{-1}(s) + \mathbf{f}_n(-s) \cdot \mathbf{f}_n{}^T(s)}{d_a(-s)d_a(s)} \tag{C5}$$

Equation (C4) indicates that LH zeroes of $det[A(s)]$ are given by

$$det[A^*(-s_{uk})] = 0 , \qquad k = 1, \ldots, k_u \tag{C6}$$

Using equations (C5) and (22b), one has

$$A^{-1}(s)\mathbf{b}(s) = C^{-1}(s)[A^*(s)]^{-1}\mathbf{f}(-s)g(s)w_{g_e}(s) \tag{C7}$$

Furthermore, since the matrix $A(s)$ has its inverse, one has an expression

$$A^{-1}(s) = P^{-1}(s)[P^T(-s)]^{-1} = C^{-1}(s)[A^*(s)]^{-1}C^{-1}(-s)$$

(see eqs. (B4) and (C4)). This suggests that $P^{-1}(s)$, and hence $\mathbf{v}(s)$ too (see eq. (B5)), has a LH factor $C^{-1}(s)$.

Possible Expression of $\mathbf{v}(s)$

In equation (B5), each entry of vector $[P^T(-s)]^{-1}\mathbf{b}(s)$ has the properties of $h(s)$ in Preliminary 1 above. Hence, putting

$$\left[[P^T(-s)]^{-1}\mathbf{b}(s)e^{-\tau_g s}\right]_+ = [P^T(-s)]^{-1}\mathbf{b}(s)e^{-\tau_g s} - \zeta(s) \tag{C8}$$

and substituting into equation (B5), one has a possible expression for $\mathbf{v}(s)$ such that

$$\mathbf{v}(s) = A^{-1}(s)\mathbf{b}(s)e^{-\tau_g s} - C^{-1}(s)\boldsymbol{\rho}(s) \tag{C9}$$

where

$$C^{-1}(s)\boldsymbol{\rho}(s) = P^{-1}(s)\zeta(s) \tag{C10}$$

is a rational polynomial vector that is again strictly proper. Following Preliminary 2, the LH factor $C^{-1}(s)$ has been artificially inserted in equation (C9). Once the unknown vector $\boldsymbol{\rho}(s)$ is determined, $\mathbf{v}(s)$ is readily solved from equation (C9). Substituting equation (C9) into equation (21), the W-H equation requires

$$[\mathbf{z}(s)]_+ = -[A(s)C^{-1}(s)\boldsymbol{\rho}(s)]_+ = \mathbf{0} \tag{C11}$$

Properties of $\rho(s)$

The unknown vector $\boldsymbol{\rho}(s)$ has the following properties.

1. In order that $\mathbf{v}(s)$ in equation (C9) be analytic in the RH s-plane, any singularity of $A^{-1}(s)\mathbf{b}(s)e^{-\tau g s}$ in the RH s-plane must vanish with its counterpart in $C^{-1}(s)\boldsymbol{\rho}(s)$. This implies that RH poles of $\boldsymbol{\rho}(s)$ must exactly coincide with those of $A^{-1}(s)\mathbf{b}(s)$ with the correct multiplicity.

2. In order that equation (C11) be valid, that is, $\mathbf{z}(s)$ be analytic in the LH s-plane, LH poles of $C^{-1}(s)\boldsymbol{\rho}(s)$ are nothing but LH zeroes of $det[A(s)]$. This fact (ref. 17) is proved as follows. Suppose $C^{-1}(s)\boldsymbol{\rho}(s)$ has a pole $s = -s_1$ with $Re(s_1) > 0$. Then after partial fraction expansion, $C^{-1}(s)\boldsymbol{\rho}(s)$ has a term $\boldsymbol{\rho}_1/(s + s_1)$ with uniquely determined coefficient vector $\boldsymbol{\rho}_1$. Executing the $[\ ]_+$ operation in equation (C11) gives

$$A(-s_1) \cdot \boldsymbol{\rho}_1 = \mathbf{0} \tag{C12}$$

which insists, for $\boldsymbol{\rho}_1 \neq \mathbf{0}$, that $det[A(-s_1)] = 0$, or equivalently, that

$$det[A^*(-s_1)] = 0 \tag{C13}$$

The statement is then proved by comparing equations (C13) and (C6). If s_1 coincides with a pole of $A(s)$, a slightly modified proof leads to the same result.

Poles of $\rho(s)$

Properties (1) and (2) determine uniquely the explicit form of $\boldsymbol{\rho}(s)$; the details are presented in the following. When $C(s)$ and $\mathbf{f}(s)$ are given by equations (11) and (6), equation (C5) becomes

$$A^*(s) = \frac{\begin{bmatrix} \left(\dfrac{\lambda_f}{\mu_f}\right)^2 \bar{d}_{cf}\, d_{cf}\, \bar{d}_a\, d_a + \bar{f}_n f_n & \bar{f}_n e_n \\ f_n \bar{e}_n & \left(\dfrac{\lambda_e}{\mu_e}\right)^2 \bar{d}_{ce}\, d_{ce}\, \bar{d}_a\, d_a + \bar{e}_n e_n \end{bmatrix}}{\bar{d}_a\, d_a} \tag{C14}$$

where $d_{cf/e} = (s + \mu_{f/e})$, $d_a = d_a(s)$, $\bar{d}_a = d_a(-s)$, etc., are used for shorthand notation. Also,

$$det[A^*(s)] = \frac{\nu^2 d_u(-s) \cdot d_u(s)}{d_a(-s) \cdot d_a(s)} \tag{C15}$$

where

$$\nu^2 d_u(-s) \cdot d_u(s) = \left(\frac{\lambda_f}{\mu_f}\right)^2 \left(\frac{\lambda_e}{\mu_e}\right)^2 \bar{d}_{cf}\, d_{cf}\, \bar{d}_{ce}\, d_{ce}\, \bar{d}_a\, d_a + \left(\frac{\lambda_f}{\mu_f}\right)^2 \bar{d}_{cf}\, d_{cf}\, \bar{e}_n e_n + \left(\frac{\lambda_e}{\mu_e}\right)^2 \bar{d}_{ce}\, d_{ce}\, \bar{f}_n f_n \tag{C16}$$

and where, with LH zeroes $s = -s_{uk}$ ($k = 1, \ldots, k_u$), $d_u(s)$ is so factored that

$$d_u(s) = \prod_{k=1}^{k_u} (s + s_{uk}) \ , \qquad k_u = i_a + 2 \tag{C17}$$

It must be noted that

$$rank[d_a(-s) d_a(s) A^*(s)]_{s = -s_{ai}} = 1 \ ; \qquad i = 1, \ldots, i_a \tag{C18}$$

which is a consequence of the fact that the output variable $y(s)$ is a scalar in this case.

Again, when $C(s)$, $\mathbf{f}(s)$ and $g(s)$ are given by equations (11) and (6), then equation (C7) is given by

$$A^{-1}(s)\mathbf{b}(s) = C^{-1}(s) \frac{\begin{bmatrix} \left(\frac{\lambda_e}{\mu_e}\right)^2 \bar{d}_{ce}\, d_{ce}\, \bar{f}_n \\ \left(\frac{\lambda_f}{\mu_f}\right)^2 \bar{d}_{cf}\, d_{cf}\, \bar{e}_n \end{bmatrix} g_n(s)}{\nu^2 d_u(-s) d_u(s)} w_{g_e}(s) \tag{C19}$$

Using equation (19a) and expanding equation (C19) into partial fractions, an alternate form

$$A^{-1}(s)\mathbf{b}(s) = C^{-1}(s)\left[\sum_{k=1}^{k_u}\left(\frac{\beta_{ok}}{-s + s_{uk}} + \frac{\gamma_{ok}}{s + s_{uk}}\right) + \frac{\eta_1}{s + \omega_g} + \frac{\eta_2}{(s + \omega_g)^2}\right] \tag{C20}$$

is obtained with unique coefficients β_{ok} and γ_{ok} (either real or complex conjugate), and η_1 and η_2 (real). Equation (C19) or (C20) indicates that only $s = s_{uk}$, $k = 1, \ldots, k_u$, are left as RH poles of $A^{-1}(s)\mathrm{b}(s)$. This is a result of hidden pole-zero cancellation. Finally, considering the properties of $\rho(s)$, one can put

$$\rho(s) = \sum_{k=1}^{k_u}\left(\frac{\beta_{pk}}{-s + s_{uk}} + \frac{\gamma_{pk}}{s + s_{uk}}\right) \tag{C21}$$

with real (for real s_{uk}) or complex conjugate (for complex conjugate s_{uk}) unknown coefficients β_{pk} and γ_{pk}, both being two dimensional (f- and e-components) vectors. There is a total of $2\times2\times k_u$ unknowns to be determined.

Unknown Coefficients β_{pk}

Applying property (1) to equation (C9) at $s = s_{uk}$, that is, requiring that $[\mathbf{v}(s) \cdot (-s + s_{uk})]_{s=s_{uk}} = 0$ with $\mathbf{v}(s)$ of equation (C9) and with $\rho(s)$ of equation (C21), one obtains

$$\beta_{pk} = [C(s)A^{-1}(s)\mathbf{b}(s)(-s + s_{uk})e^{-\tau_g s}]_{s=s_{uk}} \tag{C22}$$

When equation (C20) is substituted into equation (C22), it gives $2\times k_u$ unknown coefficients β_{pk} such as

$$\beta_{pk} = \beta_{ok}\, e^{-\tau_g s_{uk}}, \qquad k = 1, \ldots, k_u \tag{C23}$$

which depend upon τ_g.

Unknown Coefficients γ_{pk}

Applying property (2), equation (C11) must be evaluated at all LH poles of $A(s)C^{-1}(s)\rho(s)$, as shown below. At $s = -s_{uk}$, $k = 1, \ldots, k_u$

$$[A(s)C^{-1}(s)]_{s = -s_{uk}} \cdot \gamma_{pk} = 0 \tag{C24a}$$

at $s = -s_{ai}$, $i = 1, \ldots, i_a$

$$[(s + s_{ai})A(s)C^{-1}(s)\rho(s)]_{s = -s_{ai}} = 0 \tag{C24b}$$

and at $s \to -\infty$

$$[A(s)C^{-1}(s)\rho(s)]_{s \to -\infty} = 0 \tag{C24c}$$

Equations (C24a), (C24b), and (C24c) are necessary and sufficient to solve for the γ_{pk}. This becomes clear from the following notes. Equation (C24a) is simplified to $A^*(-s_{uk}) \cdot \gamma_{pk} = 0$, but it degenerates into $1\times k_u$ independent equations due to equation (C6). Hence, taking the first row of $A^*(s)$ gives, for $k = 1, \ldots, k_u$,

$$\left[\left(\frac{\lambda_f}{\mu_f}\right)^2 \bar{d}_{cf}\, d_{cf}\, \bar{d}_a\, d_a + \bar{f}_n f_n \qquad \bar{f}_n e_n\right]_{s = -s_{uk}} \cdot \gamma_{pk} = 0 \tag{C25a}$$

Next, equation (C24b) insists that $[(s + s_{ai})A^*(s)\rho(s)]_{s = -s_{ai}} = 0$, but due to equation (C18), it again degenerates into $1\times i_a$ independent relations. Taking again the first row of $A^*(s)$, one has $\mathbf{f}_n^T(-s_{ai}) \cdot \rho(-s_{ai}) = 0$, or more precisely, for $i = 1, \ldots, i_a$,

$$\mathbf{f}_n^T(-s_{ai}) \sum_{k=1}^{k_u} \frac{\gamma_{pk}}{s_{ai} - s_{uk}} = \mathbf{f}_n^T(-s_{ai}) \sum_{l=1}^{k_u} \frac{\beta_{ol}}{s_{ai} + s_{ul}}\, e^{-\tau_g s_{ul}} \tag{C25b}$$

Finally, equation (C24c) is simplified into

$$\sum_{k=1}^{k_u} \gamma_{pk} = \sum_{l=1}^{k_u} \beta_{ol}\, e^{-\tau_g s_{ul}} \tag{C25c}$$

Equations (C25a), (C25b), and (C25c) are $k_u + i_a + 2 = 2\times k_u$ independent, linear and inhomogeneous equations, and determine $2\times k_u$ unknown coefficients γ_{pk} uniquely with τ_g as a parameter.

Decomposition of $\mathbf{v}(s)$

Substituting equations (C20), (C21), and (C23) into equation (C9), one has the solution

$$\mathbf{v}(s) = C^{-1}(s)\left\{\left[\sum_{k=1}^{k_u}\left(\frac{\beta_{ok}}{-s + s_{uk}} + \frac{\gamma_{ok}}{s + s_{uk}}\right) + \frac{\eta_1}{s + \omega_g} + \frac{\eta_2}{(s + \omega_g)^2}\right] e^{-\tau_g s}\right.$$

$$\left. -\sum_{k=1}^{k_u}\left[\frac{\beta_{ok}\ e^{-\tau_g s_{uk}}}{-s + s_{uk}} + \frac{\gamma_{pk}(\tau_g)}{s + s_{uk}}\right]\right\} \tag{C26}$$

When equations (C25a), (C25b), and (C25c) are solved for $\tau_g = 0$, $\gamma_{pk}(0) = \gamma_{pk}(\tau_g = 0)$ is obtained. Using $\gamma_{pk}(0)$, equation (C26) is rearranged as follows:

$$\mathbf{v}(s) = C^{-1}(s)[\mathbf{p}_o(s)e^{-\tau_g s} + \mathbf{p}_p(s;\tau_g)] \tag{C27}$$

where

$$\mathbf{p}_o(s) = \frac{\eta_1}{s + \omega_g} + \frac{\eta_2}{(s + \omega_g)^2} + \sum_{k=1}^{k_u}\frac{\gamma_{ok} - \gamma_{pk}(0)}{s + s_{uk}}$$

$$\equiv \frac{\mathbf{p}_{on}(s)}{(s + \omega_g)^2\ d_u(s)} \tag{C28a}$$

and

$$\mathbf{p}_p(s;\tau_g) = \sum_{k=1}^{k_u}\left[\beta_{ok}\ \frac{e^{-\tau_g s} - e^{-\tau_g s_{uk}}}{-s + s_{uk}} + \frac{\gamma_{pk}(0)e^{-\tau_g s} - \gamma_{pk}(\tau_g)}{s + s_{uk}}\right]. \tag{C28b}$$

Clearly, $\mathbf{p}_o(s)$ is invariant in τ_g, and $\mathbf{p}_p(s;\tau_g) \to 0$ when $\tau_g \to 0$. Also it is not difficult to show that $\mathbf{p}_o(s)$ is obtained by directly taking the $[\ ]_+$ part in equation (C8) when $\tau_g = 0$, which is the procedure used in references 16 and 17.

System Response $g_u(s)$

Let us consider the system response $g_u(s)$ of equation (14) with the feed-forward loop closed, which is now decomposed as

$$g_u(s) = g_{uo}(s) + g_{up}(s) \tag{C29}$$

where

$$g_{uo}(s) = g(s) - \mathbf{f}^T(s)\mathbf{p}_o(s)w_{ge}^{-1}(s) \tag{C30a}$$

$$g_{up}(s) = -\mathbf{f}^T(s)\mathbf{p}_p(s;\tau_g)w_{ge}^{-1}(s)e^{\tau_g s} \tag{C30b}$$

Apparently, both $g_{uo}(s)$ and $g_{up}(s)$ have a factor $d_a(s)$ in their denominators; these factors are cancelled out with numerators. This is shown as follows. Since $C^{-1}(s)\mathbf{p}_o(s)$ is a part of $\mathbf{v}(s)$ when $\tau_g = 0$, and hence satisfies the Wiener-Hopf equation (see eq. (21)),

$$[A(s)C^{-1}(s)\mathbf{p}_o(s) - \mathbf{b}(s)]_+ = \mathbf{0} \tag{C31}$$

Executing the $[\ ]_+$ operation at $s = -s_{ai}$, $i = 1, \ldots, i_a$, reveals that

$$\Big[[\mathbf{f}^T(s)\mathbf{p}_o(s) - g(s)w_{ge}(s)](s + s_{ai})\Big]_{s = -s_{ai}} = 0 \tag{C32}$$

which assures that the factor $d_a(s)$ in the common denominator of equation (C30a) is cancelled out by its numerator. Thus, one can rearrange equation (C30a) as

$$g_{uo}(s) = \frac{g_{uon}(s)}{\left(s + \frac{\omega_g}{\sqrt{3}}\right) d_u(s)} \tag{C33}$$

where $g_{uon}(s)$ is a polynomial in s, the order of which is not greater than that of $(s + \omega_g/\sqrt{3}) \cdot d_u(s)$. Next, $g_{up}(s)$ of equation (C30b) has a factor

$$\mathbf{f}^T(s)\mathbf{p}_p(s;\tau_g) = \frac{\mathbf{f}_n^T(s)}{d_a(s)} \sum_{k=1}^{k_u} \left\{ \left[\frac{\beta_{ok}}{-s + s_{uk}} + \frac{\gamma_{pk}(0)}{s + s_{uk}} \right] e^{-\tau_g s} - \left[\frac{\beta_{pk}}{-s + s_{uk}} + \frac{\gamma_{pk}(\tau_g)}{s + s_{uk}} \right] \right\} \tag{C34}$$

By virtue of equation (C25b), it can be shown that equation (C34) is finite at $s = -s_{ai}$, and $i = 1, \ldots, i_a$, which means that the denominator $d_a(s)$ in $\mathbf{f}^T(s)$ is cancelled by the same factor in the numerator of $g_{up}(s)$. Thus, one has a form

$$g_{up}(s) = -\sum_{k=1}^{k_u}\left[\mathbf{f}^T(s_{uk}) \cdot \beta_{ok}\,\frac{1 - e^{-\tau_g s_{uk}}\, e^{\tau_g s}}{-s + s_{uk}}\right.$$

$$\left. + \mathbf{f}^T(-s_{uk})\,\frac{\gamma_{pk}(0) - \gamma_{pk}(\tau_g)e^{\tau_g s}}{s + s_{uk}}\right] w_{g_e}^{-1}(s) \qquad \text{(C35)}$$

Filter Gains

The following is obtained after straightforward manipulations. As to the basic part of the filter, partial fraction expansion of equation (29) with a substitution of equation (C28a) results in

$$\mathbf{c}_o = \frac{1}{c_{g_e}}\begin{pmatrix} \frac{1}{\mu_f} & 0 \\ 0 & \frac{1}{\mu_e} \end{pmatrix}\left\{\eta_2 + \left(1 - \frac{1}{\sqrt{3}}\right)\omega_g \eta_1\right.$$

$$\left. + \sum_{k=1}^{k_u}\left[\gamma_{ok} - \gamma_{pk}(0)\right]\left[\left(2 - \frac{1}{\sqrt{3}}\right)\omega_g - s_{uk}\right]\right\} \qquad \text{(C36a)}$$

$$\mathbf{c}_w = \frac{1}{c_{g_e}}\begin{pmatrix} 1 - \frac{\omega_g}{\sqrt{3}\ \mu_f} & 0 \\ 0 & 1 - \frac{\omega_g}{\sqrt{3}\ \mu_e} \end{pmatrix}\left[\eta_2 + \left(1 - \frac{1}{\sqrt{3}}\right)\omega_g \eta_1\right.$$

$$\left. + \left(1 - \frac{1}{\sqrt{3}}\right)^2 \omega_g^{\,2} \sum_{k=1}^{k_u} \frac{\gamma_{ok} - \gamma_{pk}(0)}{s_{uk} - \omega_g/\sqrt{3}}\right] \qquad \text{(C36b)}$$

$$\mathbf{c}_k = \frac{1}{c_{g_e}}\begin{pmatrix} 1 - \frac{s_{uk}}{\mu_f} & 0 \\ 0 & 1 - \frac{s_{uk}}{\mu_e} \end{pmatrix} \cdot \frac{(\omega_g - s_{uk})^2}{\frac{\omega_g}{\sqrt{3}} - s_{uk}} \cdot \left[\gamma_{ok} - \gamma_{pk}(0)\right] \qquad \text{(C36c)}$$

where $\mathbf{c}_o$ and $\mathbf{c}_w$ are real, and $\mathbf{c}_k$ is either real or complex conjugate. The same procedure is executed for the additional part of equation (32), and then one has

$$\mathbf{l}_k(\tau_g) = -\frac{1}{c_{g_e}} \begin{pmatrix} \frac{1}{\mu_f} & 0 \\ 0 & \frac{1}{\mu_e} \end{pmatrix} \cdot s_{uk} \cdot \left[\gamma_{pk}(\tau_g) + \beta_{ok}\, e^{-\tau_g s_{uk}}\right] \tag{C37a}$$

$$\mathbf{r}_k = \frac{1}{c_{g_e}} \begin{pmatrix} 1 + \frac{s_{uk}}{\mu_f} & 0 \\ 0 & 1 + \frac{s_{uk}}{\mu_e} \end{pmatrix} \cdot \frac{(\omega_g + s_{uk})^2}{s_{uk} + \frac{\omega_g}{\sqrt{3}}} \cdot \beta_{ok} \tag{C37b}$$

$$\mathbf{t}_k(\tau_g) = \frac{1}{c_{g_e}} \left(1 - \frac{1}{\sqrt{3}}\right)^2 \omega_g^{\,2} \begin{pmatrix} 1 - \frac{s_{uk}}{\mu_f} & 0 \\ 0 & 1 - \frac{s_{uk}}{\mu_e} \end{pmatrix}$$

$$\times \left[\frac{\beta_{ok}\, e^{-\tau_g s_{uk}}}{s_{uk} + \frac{\omega_g}{\sqrt{3}}} + \frac{\gamma_{pk}(\tau_g)}{s_{uk} - \frac{\omega_g}{\sqrt{3}}}\right] \tag{C37c}$$

$$\mathbf{s}_k(\tau_g) = \frac{1}{c_{g_e}} \begin{pmatrix} 1 - \frac{s_{uk}}{\mu_f} & 0 \\ 0 & 1 - \frac{s_{uk}}{\mu_e} \end{pmatrix} \cdot \frac{(\omega_g - s_{uk})^2}{\frac{\omega_g}{\sqrt{3}} - s_{uk}}\, \gamma_{pk}(\tau_g) \tag{C37d}$$

where $\mathbf{l}_k$, $\mathbf{r}_k$, $\mathbf{t}_k$ and $\mathbf{s}_k$ are again either real or complex conjugate.

REFERENCES

1. Phillips, William H.: Gust Alleviation. *In* NASA, Langley Reserach Center. Performance and Dynamics of Aerospace Vehicles. NASA SP-258, 1971, pp. 505-553.

2. Barker, L. Keith; Crawford, Daniel J.; and Sparrow, Gene W.: Effect of Limited Amplitude and Rate of Flap Motion on Vane-Controlled Gust Alleviation System. NASA TN D-6733, March 1972.

3. Oehman, Waldo I.: Analytical Study of the Performance of a Gust Alleviation System for a STOL Airplane. NASA TN D-7201, April 1973.

4. Oehman, Waldo I.: Analytical Study of the Performance of a Gust Alleviation System with a Vane Sensor. NASA TN D-7431, Feb. 1974.

5. Thompson, G. O.; Eslinger, D. L.; Gordon, C. K.; and Dodson, R. O.: STOL Ride Control Feasibility Study. AIAA Paper No. 73-885, Aug. 1973.

6. Cohen, Gerald C.; Cotter, Cliff; and Taylor, Donald L.: Use of Active Control Technology to Improve Ride Qualities of Large Transport Aircraft. *In* NASA, Flight Research Center, Edwards, Calif., Advanced Control Technology and Its Potential for Future Transport Aircraft. Los Angeles, Calif., July 9-11, 1974.

7. Nakagawa, K.; Murotsu, Y.; Tsumura, T.; and Fujiwara, N.: On the Most Feasible Configuration for Airplane Gust-Alleviation System. (in Japanese), J. of Japan Soc. for Aeronaut. and Space Sci., vol. 18, no. 197, June 1970, pp. 214-222.

8. Hutin, Pierre-Marie: Une Nouvelle Méthode pour Calculer un Absorbeur de Rafales pour un Avion Souple, Utilisant un Dispositif en Boucle Ouverte. ONERA, T.P. no. 1236, 1973.

9. Stone, Ralph W., Jr.: Ride-Quality Overview. Symposium on Vehicle Ride Quality. NASA TM X-2620, Oct. 1972, pp. 1-22.

10. Barker, L. Keith: Effects of Spanwise Variation of Gust Velocity on Alleviation System Designed for Uniform Gust Velocity Across Span. NASA TN D-6346, June 1971.

11. Glaser, J. J.: Data Requirements on Turbulence in the Earth's Atmospheric Shear Layer for STOL Design Criteria. Flight in Turbulence, AGARD-CP-140, 1974, pp. 17.1-17.8.

12. Papoulis, Athanasios: Probability, Random Variables, and Stochastic Processes, N. Y., McGraw-Hill Book Co., 1965, pp. 149-151.

13. Youla, D. C.: On the Factorization of Rational Matrices. IRE Transactions on Information Theory, vol. IT-7, no. 3, July 1961, pp. 172-189.

14. Tsien, Hsue S.: Engineering Cybernetics. Chapter 16, McGraw-Hill Book Co., N. Y., 1954.

15. Freedman, Marvin I.: A Maximum-Order Theorem for Optimal Rational Models. IEEE Transactions on Automatic Control, vol. AC 18, no. 2, April 1973, pp. 172-174.

16. Whitbeck, R. F.: A Frequency Domain Approach to Linear Optimal Control. J. Aircraft, vol. 5, no. 4, July-Aug. 1968, pp. 395-401.

17. Brockett, R. W.; and Mesarović, M. D.: Synthesis of Linear Multi-Variable Systems, (American Institute of Electrical Engineers Transactions, Pt. II. Applications and Industry.) vol. 81, Sept. 1962, pp. 216-221.

18. Smetana, F. O.; Summey, D. C.; and Johnson, W. D.: Riding and Handling Qualities of Light Aircraft - A Review and Analysis. NASA CR-1975, March 1972.

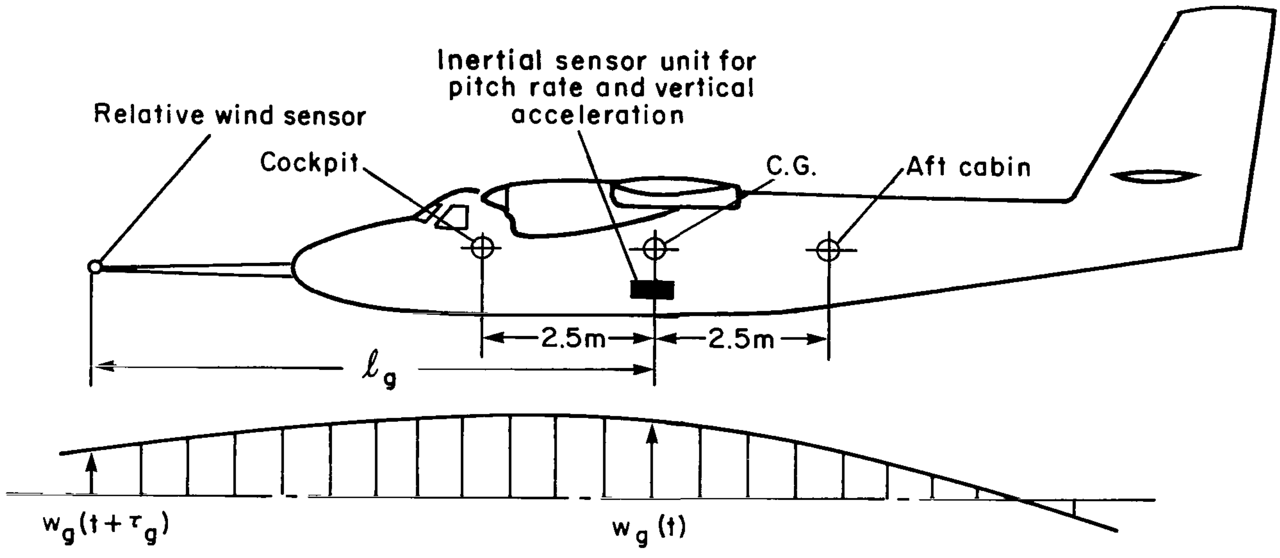

(a) Sensor and ride quality measurement stations.

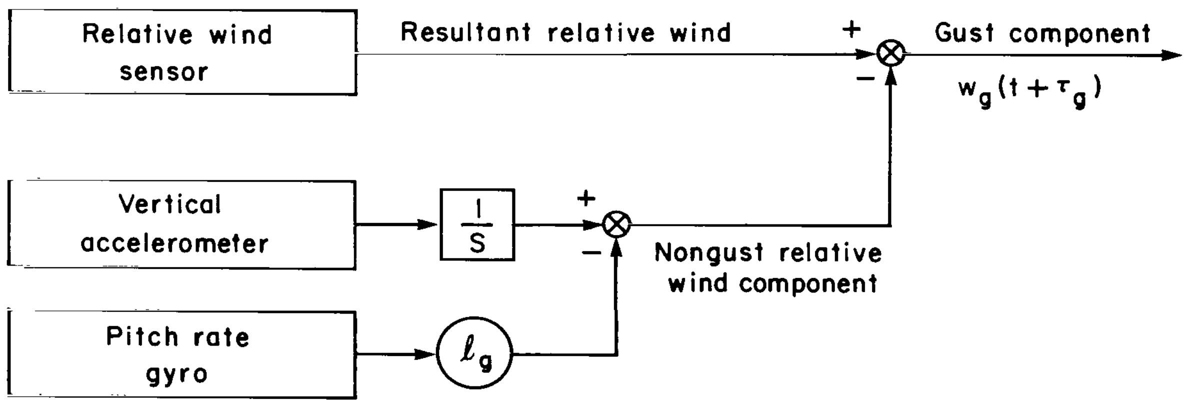

(b) Signal flow for extracting gust component.

Figure 1.- Gust alleviation system.

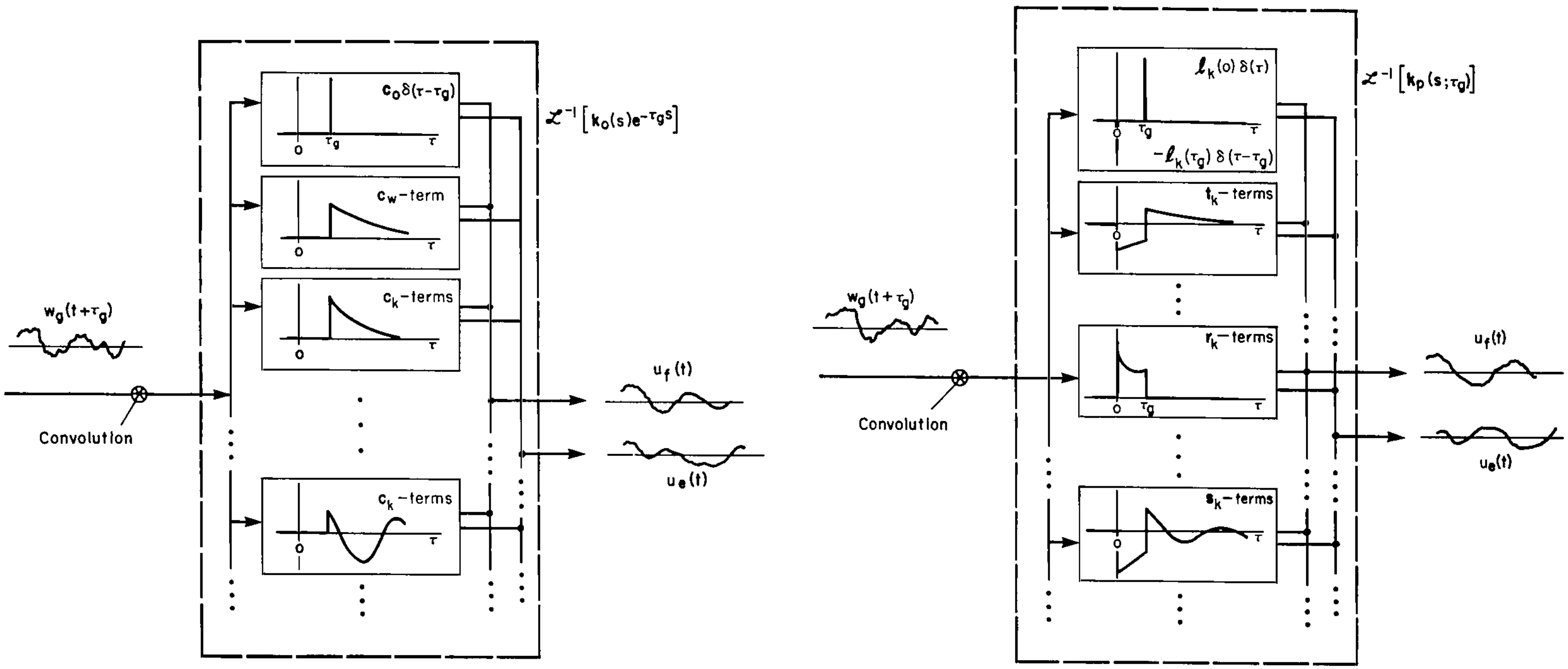

(a) Basic part $\mathbf{k}_o(s)e^{-\tau_g s}$.

(b) Additional part $\mathbf{k}_p(s;\tau_g)$.

Figure 2.- Structure of optimal filter.

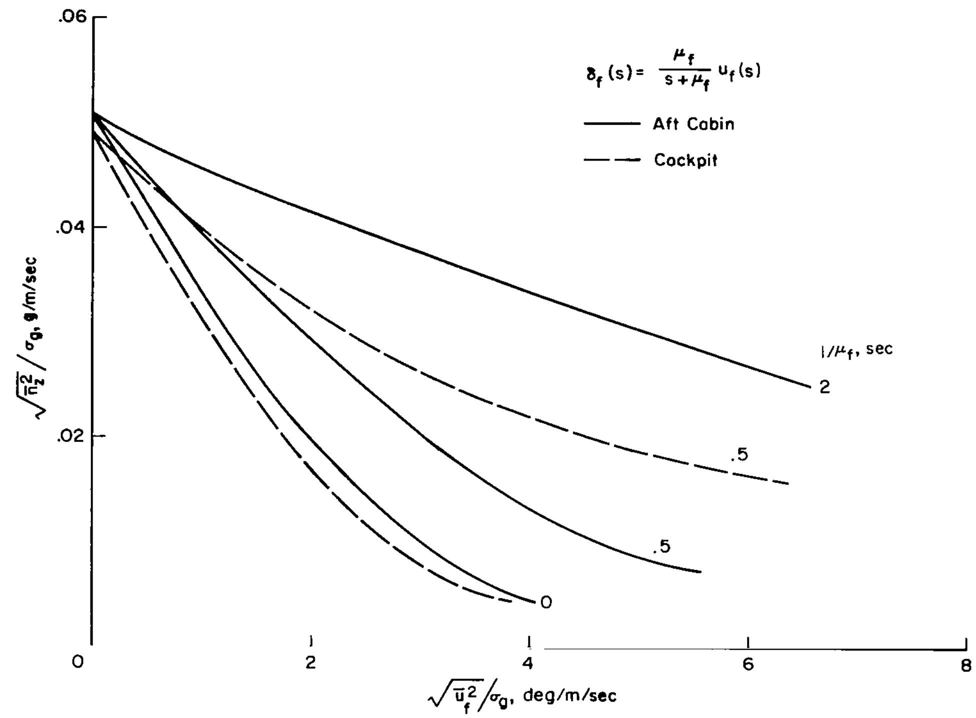

Figure 3.- Effect of flap (τ_g = 0).

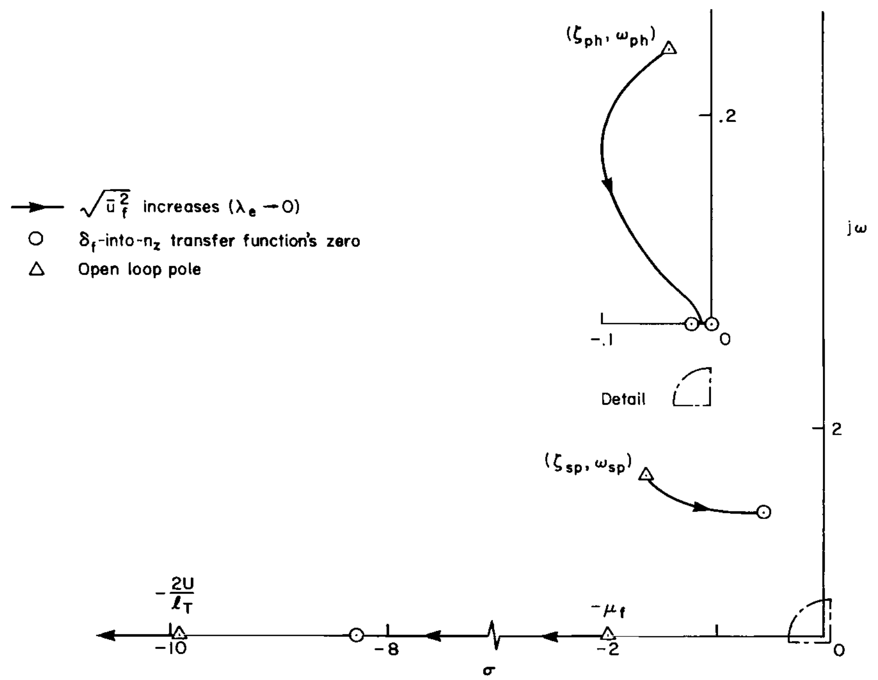

Figure 4.- Locations of system pole, flap only.

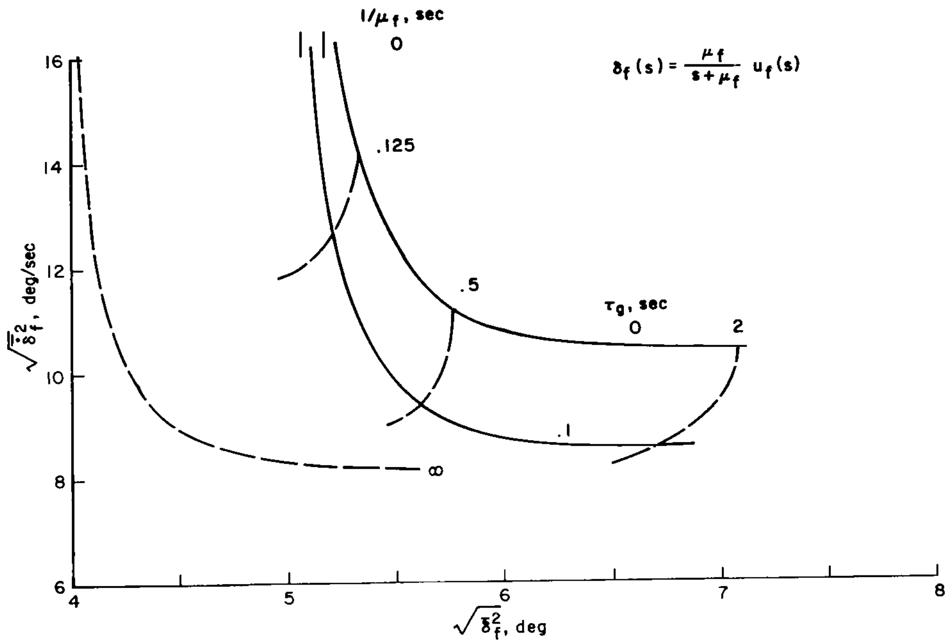

Figure 5.- Flap system tradeoff characteristics to achieve $\sqrt{\overline{n_z}^2} = 0.03$ g for $\sigma_g = 2.1$ m/sec at aft cabin station.

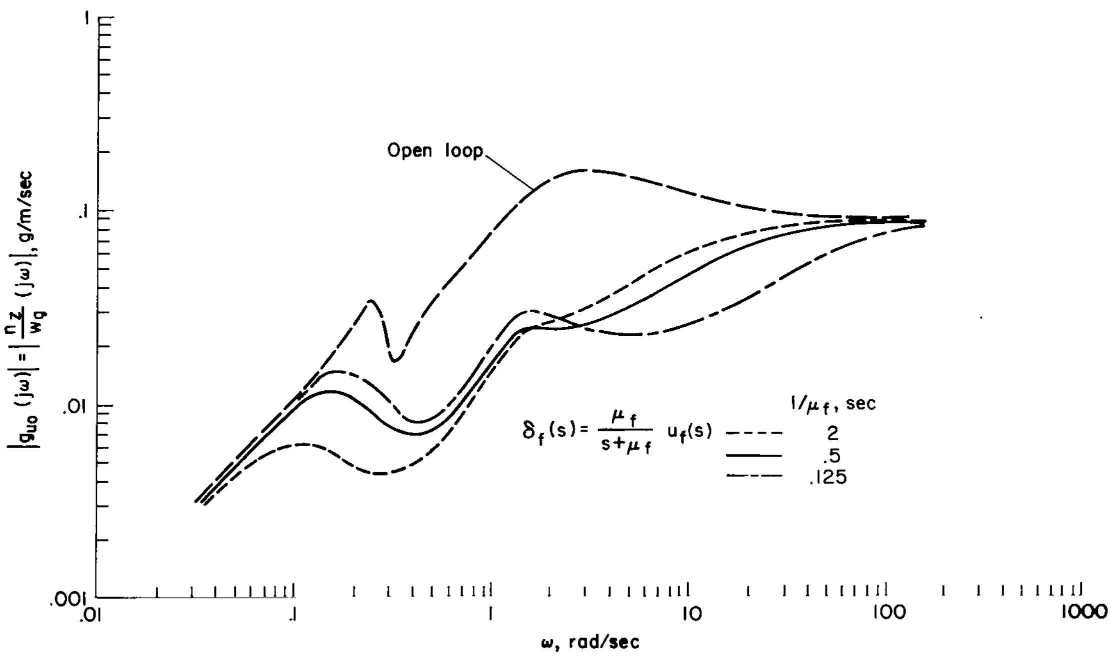

Figure 6.- System transfer function $g_{uo}(s)$ to achieve $\sqrt{\overline{n_z}^2} = 0.03$ g for $\sigma_g = 2.1$ m/sec at aft cabin station ($\tau_g = 0$).

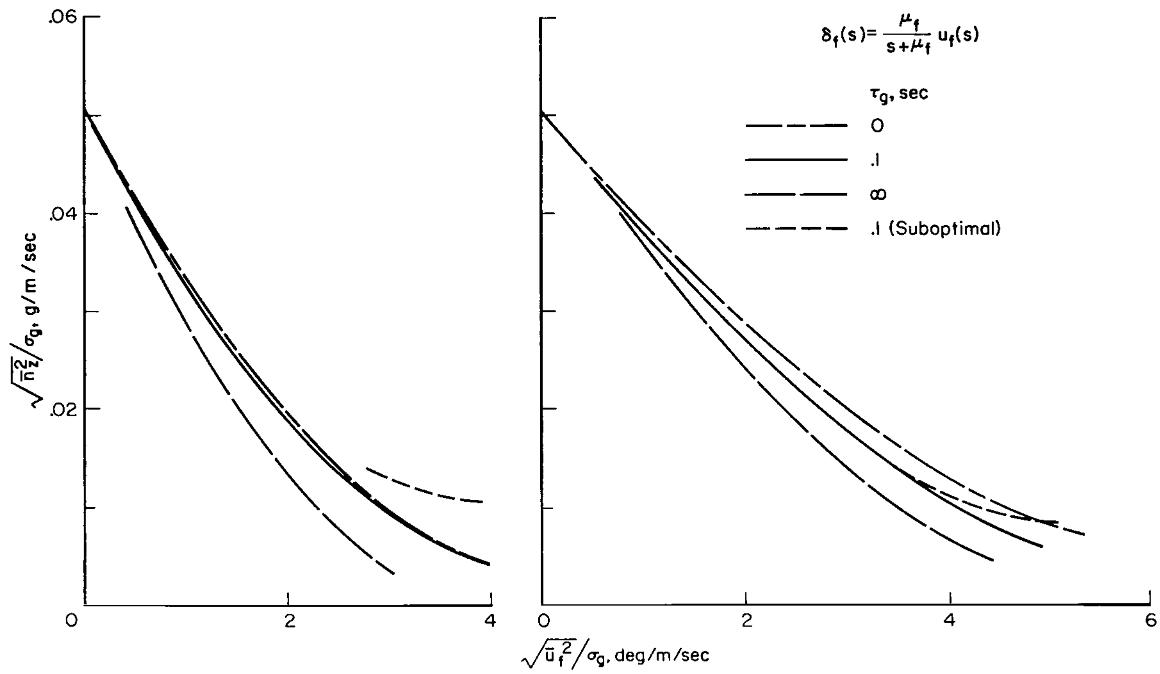

(a) $1/\mu_f = 0$ (b) $1/\mu_f = 0.5$ sec

Figure 7.- Effect of lead time on flap control (aft cabin station).

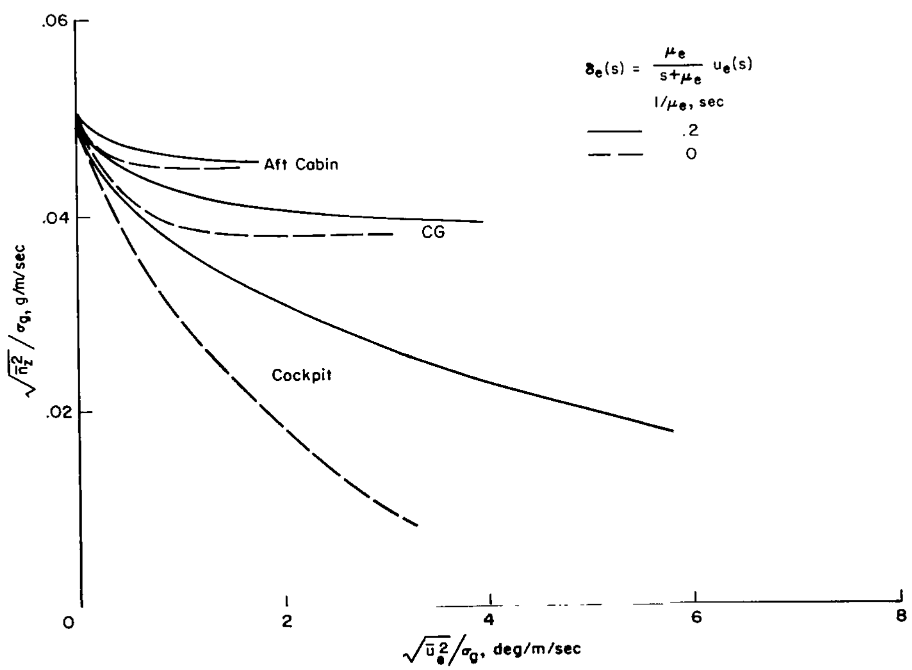

Figure 8.- Effect of elevator ($\tau_g = 0$).

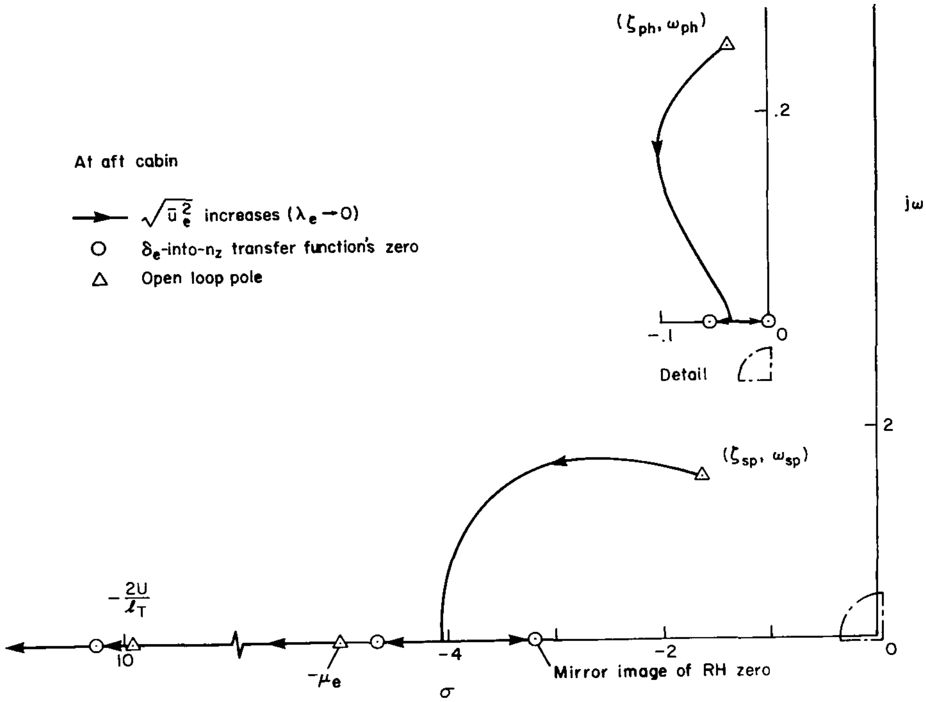

Figure 9.- Locations of system pole, elevator only.

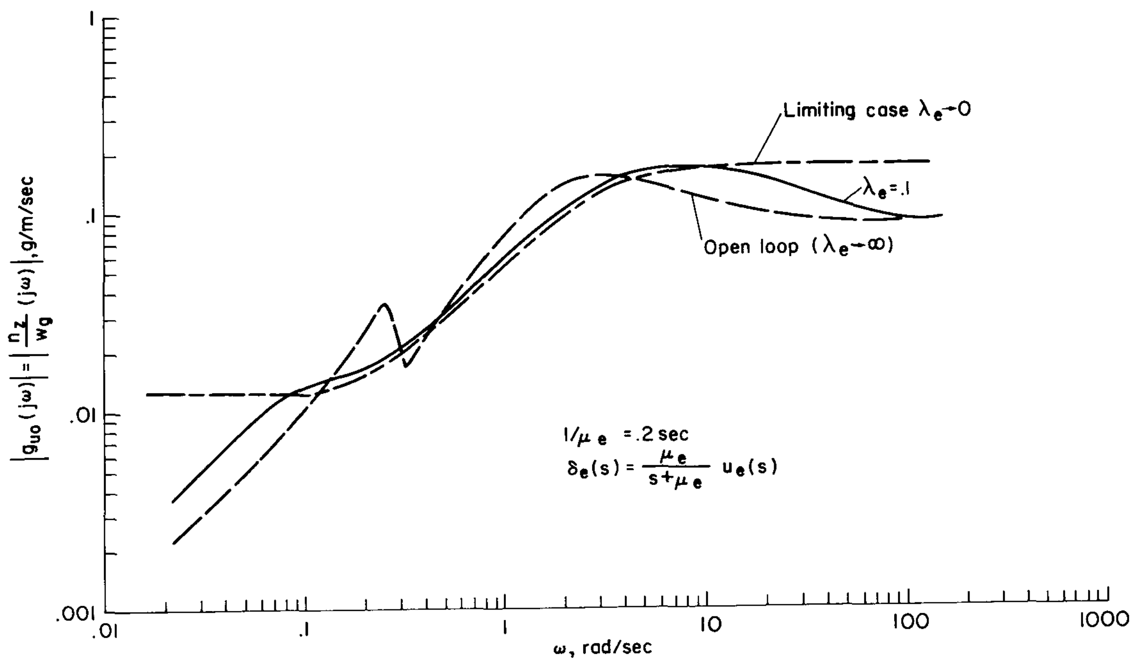

Figure 10.- System transfer function $g_{uo}(s)$ at cabin station ($\tau_g = 0$, $1/\mu_e = 0.2$ sec).

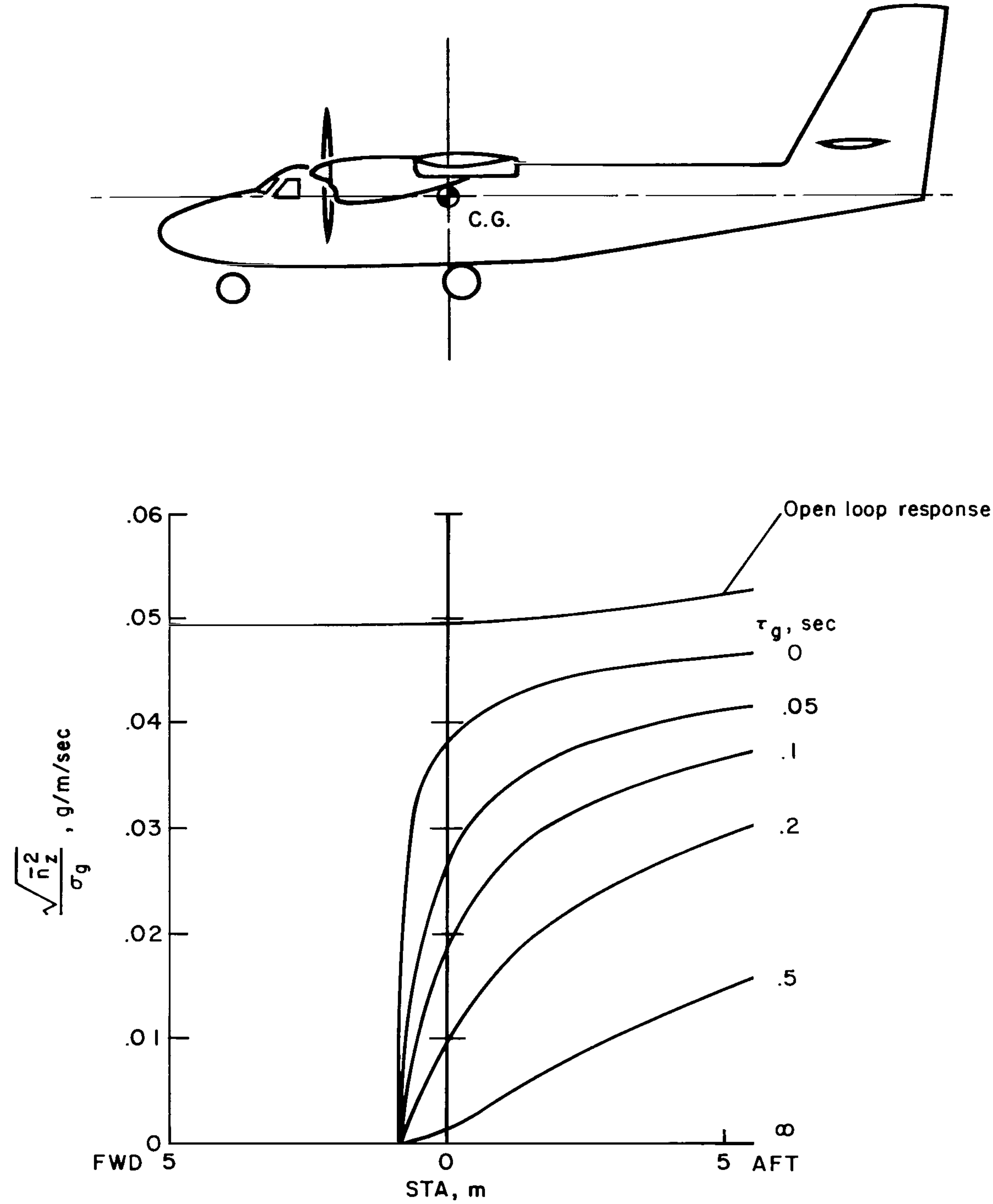

Figure 11.- Limiting performance of elevator control when $\lambda_e \to 0$ ($\sqrt{\overline{u_e^2}} \to \infty$) for $\tau_g \geq 0$.

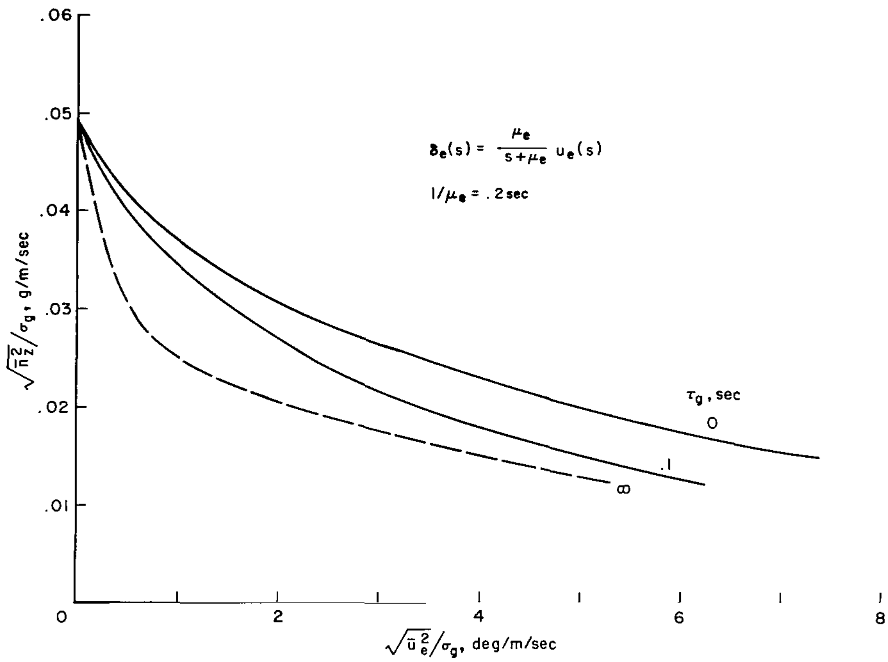

(a) Cockpit station.

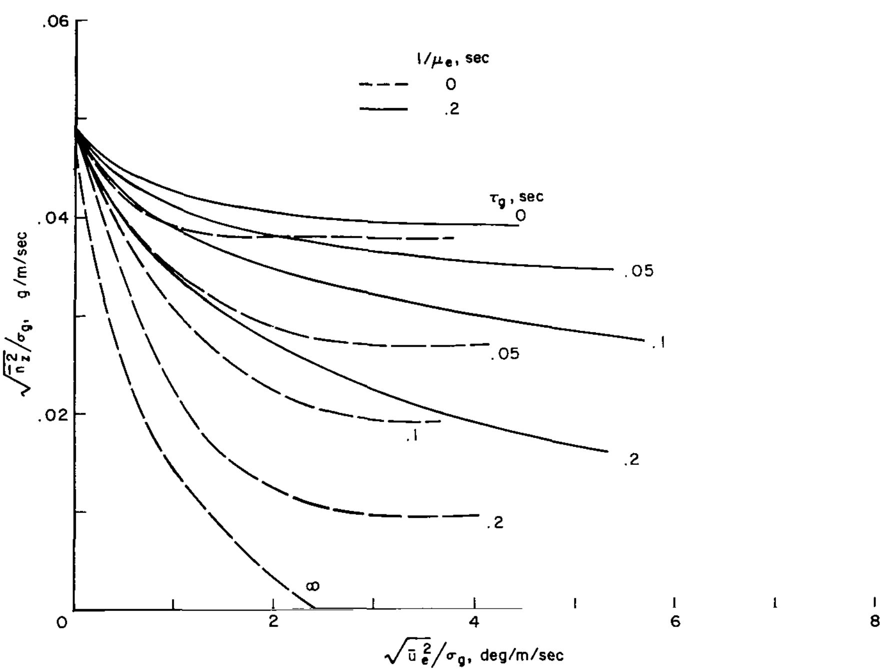

(b) CG station.

Figure 12.- Effect of lead time on elevator control.

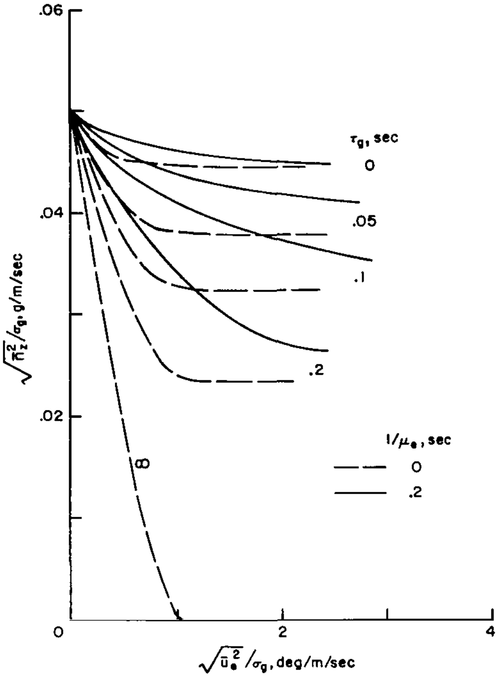

(c) Aft cabin station.

Figure 12.- Concluded.

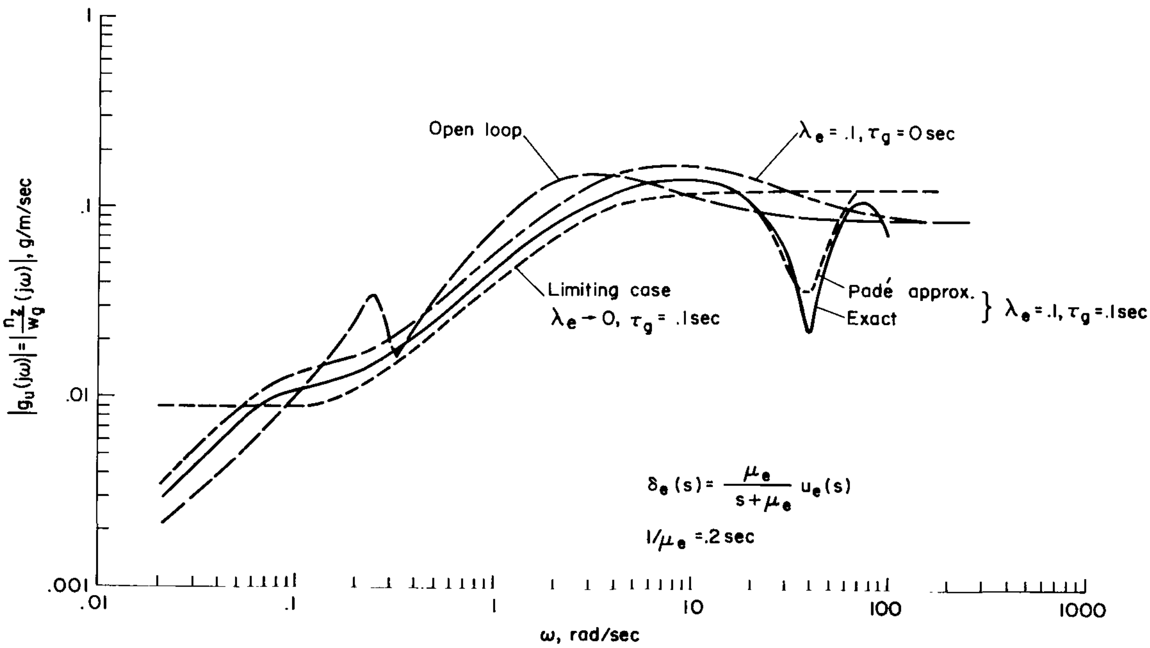

Figure 13.- System transfer function $g_u(s)$ at aft cabin station (elevator only).

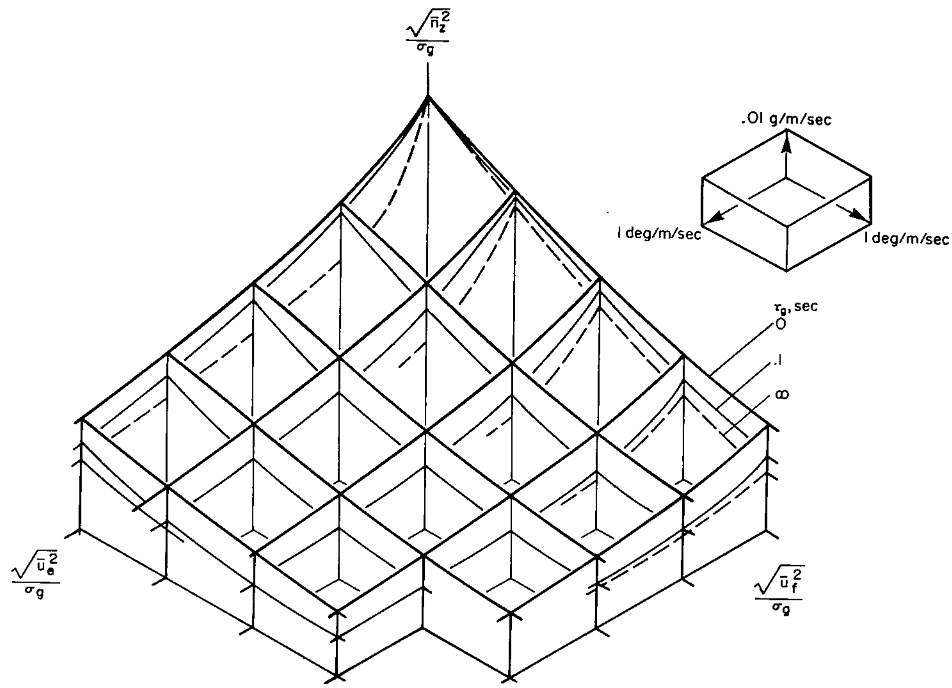

(a) Cockpit station ($1/\mu_f$ = 0.5 sec, $1/\mu_e$ = 0.2 sec).

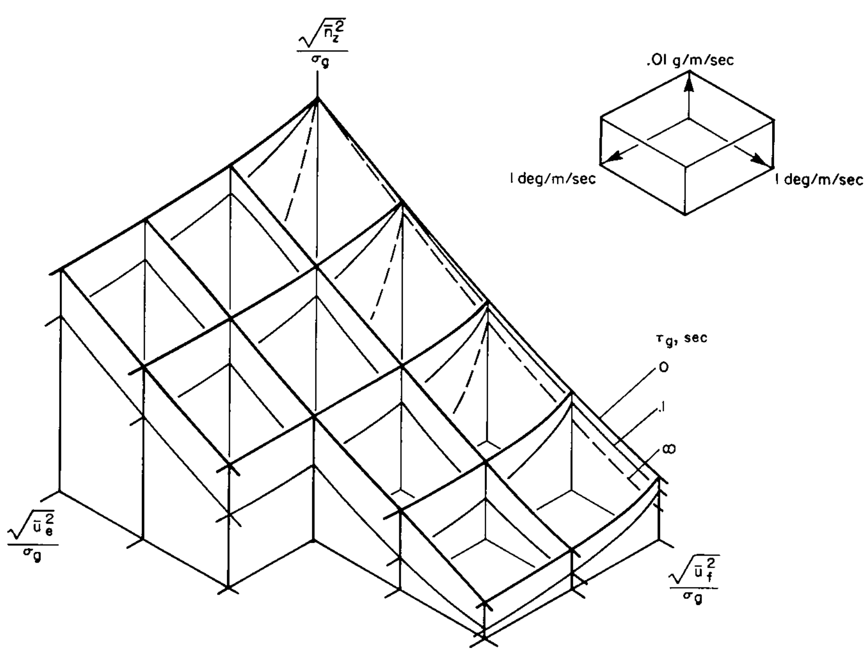

(b) Aft cabin station ($1/\mu_f$ = 0.5 sec, $1/\mu_e$ = 0.2 sec).

Figure 14.- Effect of two controllers (τ_g = 0 and τ_g > 0).

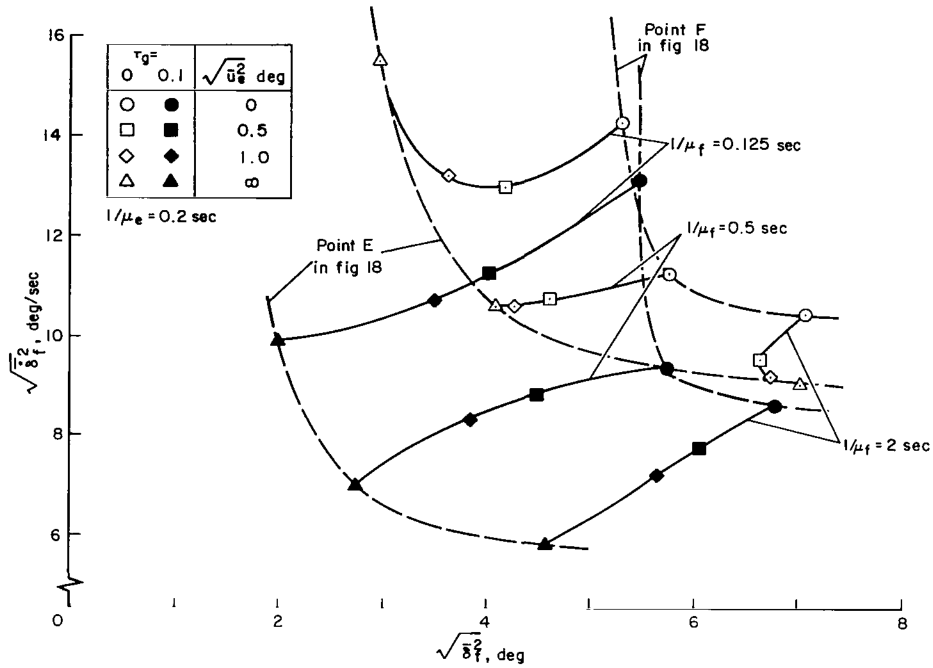

Figure 15.- Reduction of required cost in flap system due to elevator control ($\sqrt{\overline{n_z^2}}$ = 0.03 g for σ_g = 2.1 m/sec, aft cabin station).

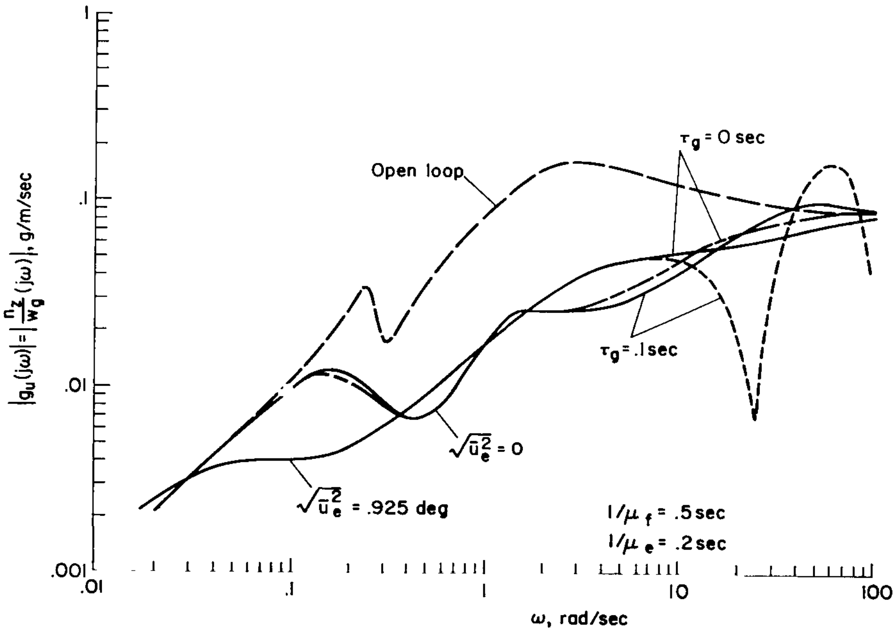

Figure 16.- System transfer function $g_u(s)$ at aft cabin station with two controllers ($\sqrt{\overline{n_z^2}}$ = 0.03 g for σ_g = 2.1 m/sec).

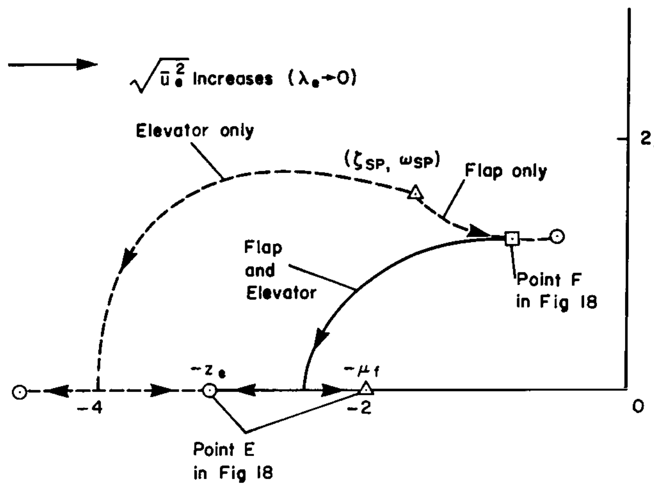

Figure 17.- Locations of system pole when two controllers are used to achieve $\sqrt{\overline{n_z^2}}$ = 0.03 g for σ_g = 2.1 m/sec.

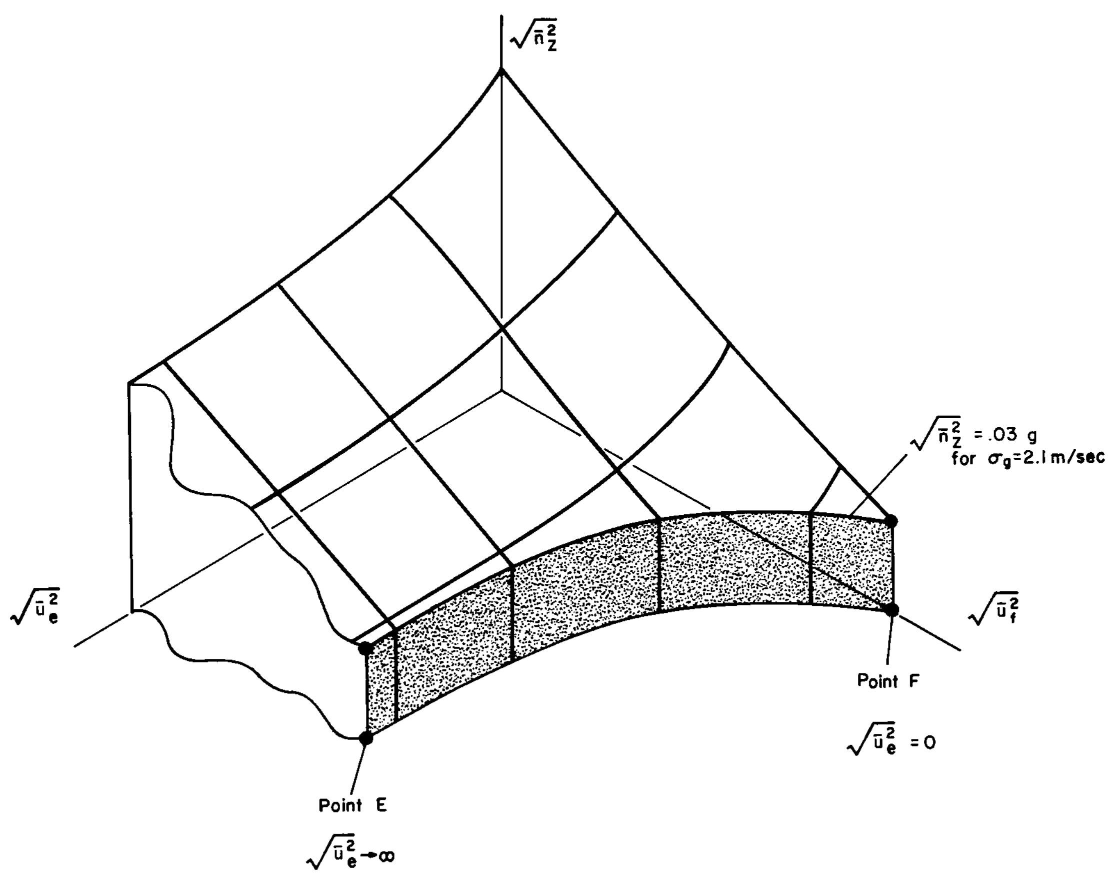

Figure 18.- Two limiting cases to achieve a given criterion of $\sqrt{\overline{n_z^2}}$.

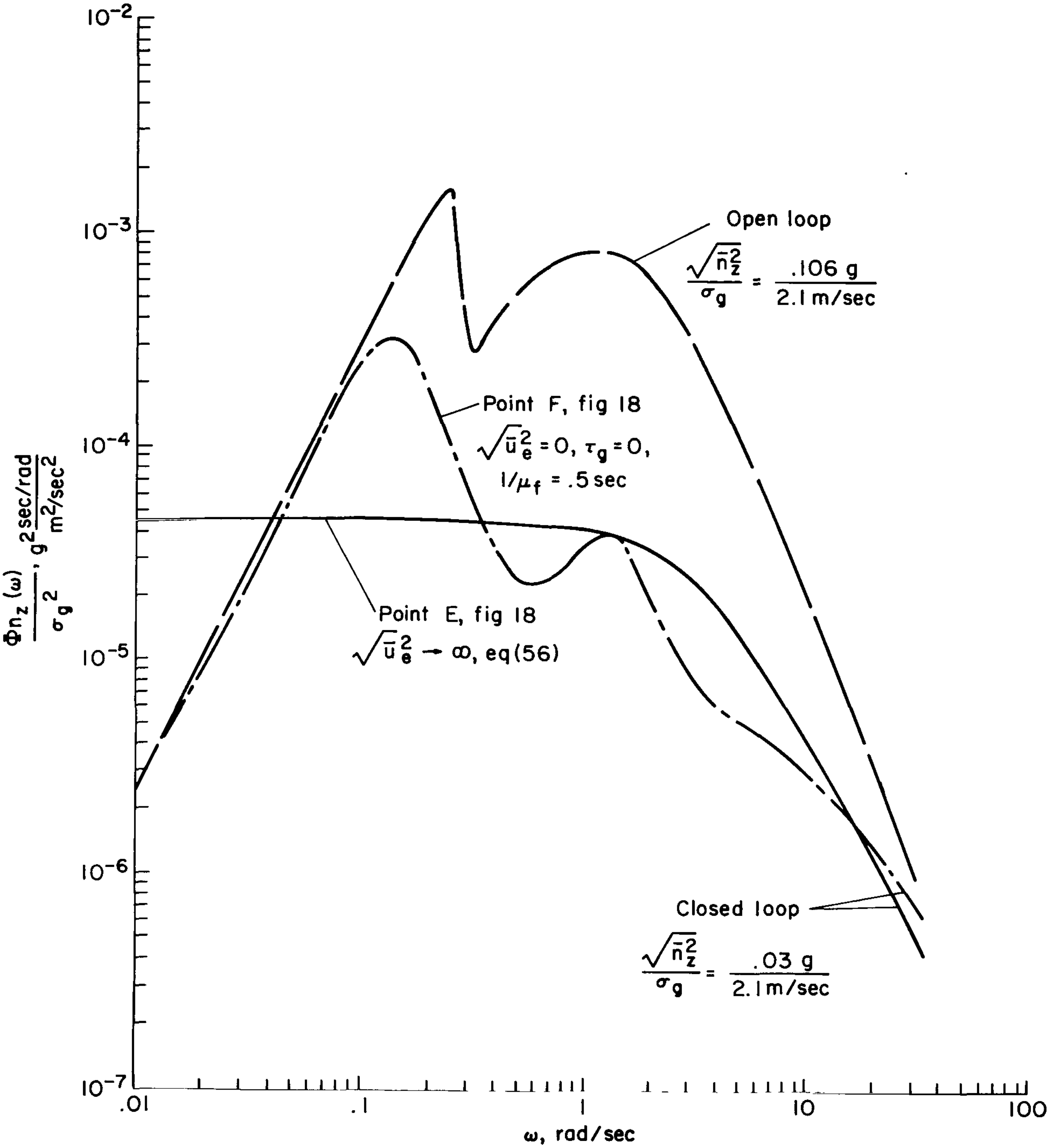

Figure 19.- Power spectra of n_z (aft cabin).

"The aeronautical and space activities of the United States shall be conducted so as to contribute . . . to the expansion of human knowledge of phenomena in the atmosphere and space. The Administration shall provide for the widest practicable and appropriate dissemination of information concerning its activities and the results thereof."

—NATIONAL AERONAUTICS AND SPACE ACT OF 1958

NASA SCIENTIFIC AND TECHNICAL PUBLICATIONS

TECHNICAL REPORTS: Scientific and technical information considered important, complete, and a lasting contribution to existing knowledge.

TECHNICAL NOTES: Information less broad in scope but nevertheless of importance as a contribution to existing knowledge.

TECHNICAL MEMORANDUMS: Information receiving limited distribution because of preliminary data, security classification, or other reasons. Also includes conference proceedings with either limited or unlimited distribution.

CONTRACTOR REPORTS: Scientific and technical information generated under a NASA contract or grant and considered an important contribution to existing knowledge.

TECHNICAL TRANSLATIONS: Information published in a foreign language considered to merit NASA distribution in English.

SPECIAL PUBLICATIONS: Information derived from or of value to NASA activities. Publications include final reports of major projects, monographs, data compilations, handbooks, sourcebooks, and special bibliographies.

TECHNOLOGY UTILIZATION PUBLICATIONS: Information on technology used by NASA that may be of particular interest in commercial and other non-aerospace applications. Publications include Tech Briefs, Technology Utilization Reports and Technology Surveys.

Details on the availability of these publications may be obtained from:

SCIENTIFIC AND TECHNICAL INFORMATION OFFICE

NATIONAL AERONAUTICS AND SPACE ADMINISTRATION

Washington, D.C. 20546